

# Met and Cxcr4 cooperate to protect skeletal muscle stem cells against inflammation-induced damage during regeneration

Ines Lahmann<sup>1,2</sup>, Joscha Griger<sup>2†</sup>, Jie-Shin Chen<sup>2‡</sup>, Yao Zhang<sup>2</sup>, Markus Schuelke<sup>3</sup>, Carmen Birchmeier<sup>1,2\*</sup>

<sup>1</sup>Neurowissenschaftliches Forschungszentrum, NeuroCure Cluster of Excellence, Charité–Universitätsmedizin Berlin, Corporate Member of Freie Universität Berlin and Humboldt-Universität zu Berlin, Berlin, Germany; <sup>2</sup>Developmental Biology/Signal Transduction Group, Max Delbrueck Center for Molecular Medicine (MDC) in the Helmholtz Society, Berlin, Germany; <sup>3</sup>Department of Neuropediatrics, Charité–Universitätsmedizin Berlin, Corporate Member of Freie Universität Berlin and Humboldt-Universität zu Berlin, Berlin, Germany

**Abstract** Acute skeletal muscle injury is followed by an inflammatory response, removal of damaged tissue, and the generation of new muscle fibers by resident muscle stem cells, a process well characterized in murine injury models. Inflammatory cells are needed to remove the debris at the site of injury and provide signals that are beneficial for repair. However, they also release chemokines, reactive oxygen species, as well as enzymes for clearance of damaged cells and fibers, which muscle stem cells have to withstand in order to regenerate the muscle. We show here that MET and CXCR4 cooperate to protect muscle stem cells against the adverse environment encountered during muscle repair. This powerful cyto-protective role was revealed by the genetic ablation of Met and Cxcr4 in muscle stem cells of mice, which resulted in severe apoptosis during early stages of regeneration. TNF $\alpha$  neutralizing antibodies rescued the apoptosis, indicating that TNF $\alpha$  provides crucial cell-death signals during muscle repair that are counteracted by MET and CXCR4. We conclude that muscle stem cells require MET and CXCR4 to protect them against the harsh inflammatory environment encountered in an acute muscle injury.

\*For correspondence: [cbirch@mdc-berlin.de](mailto:cbirch@mdc-berlin.de)

Present address: <sup>†</sup>Center for Translational Cancer, Technische Universität München, Munich, Germany; <sup>‡</sup>CVMD, IMED Biotech Unit, AstraZeneca Gothenburg, Mölndal, Sweden

Competing interest: [See page 16](#)

Funding: [See page 16](#)

Received: 29 March 2020

Accepted: 04 August 2021

Published: 05 August 2021

Reviewing Editor: Gabrielle Kardon, University of Utah, United States

© Copyright Lahmann et al. This article is distributed under the terms of the [Creative Commons Attribution License](#), which permits unrestricted use and redistribution provided that the original author and source are credited.

## Introduction

Muscle injury through trauma is common and can be repaired by muscle regeneration (*Järvinen et al., 2005; Tidball, 2005; Tidball, 2017*). Stem cells reside in the muscle tissue and provide the cellular source for the regeneration process (*Chargé and Rudnicki, 2004; Relaix and Zammit, 2012*). Muscle stem cells are characterized by the expression of PAX7 and their location in the stem cell niche between the basal lamina and plasma membrane of the muscle fiber (*Mauro, 1961; Seale et al., 2000*). Muscle stem cells are quiescent in the adult, but can be re-activated upon injury. On one hand, activated muscle stem cells proliferate and generate differentiating cells to repair the muscle, and on the other they can self-renew to repopulate the stem cell niche (*Chargé and Rudnicki, 2004; Relaix and Zammit, 2012*). A complex interplay between muscle stem cells and their environment occurs during muscle repair. Inflammatory cells and the cytokines they produce provide important cues for muscle stem cells and regulate their activation, proliferation, and differentiation. Therefore, communication between muscle stem cells and the immune system needs to be tightly regulated. Failure of

adequate communication results in incomplete regeneration as well as sustained or chronic inflammation that ultimately damages the muscle (Chazaud et al., 2009; Saclier et al., 2013b; Londhe and Guttridge, 2015; Tidball, 2017).

Shortly after an acute muscle injury, resident macrophages are activated and large numbers of macrophages and neutrophils are recruited to the injured tissue. This accumulation of immune cells is a prerequisite for the removal of damaged fibers (Tidball, 2005). The immune cells amplify the inflammatory response and create a milieu that is rich in inflammatory cytokines, reactive oxygen species, proteases, and membrane-damaging agents (Butterfield et al., 2006; Mann et al., 2011; Le Moal et al., 2017). This produces a noxious environment that muscle stem cells and regenerating fibers must withstand in order to properly rebuild functional muscle tissue. How muscle stem cells are protected from these noxious cues has not yet been elucidated.

We reasoned that investigating the direct role of cytokines on muscle stem cells and during muscle repair after acute injury will help to define factors that could be beneficial in a therapeutic setting. We used cardiotoxin injection as our muscle injury model that resulted in widespread necrosis of muscle fibers, massive infiltration by neutrophils and macrophages followed by myogenic regeneration. In such a setting, extensive proliferation of muscle stem cells occurs, amplifying their numbers and providing the cellular material for new myofibers (Hardy et al., 2016). Nevertheless, a substantial number of stem cells are lost during the acute inflammatory response (Hardy et al., 2016).

We show here that endogenous cytokines enable muscle stem cells to survive in the noxious environment encountered after injury. We used mouse genetics to demonstrate that MET/HGF and CXCR4/CXCL12 signals cooperate to protect muscle stem cells during early stages of regeneration. We identify TNF $\alpha$  as a factor that damages the stem cells in this setting. Together, our study shows that inflammatory factors have dual effects, damaging (TNF $\alpha$ ) and protecting (HGF and CXCL12) muscle stem cells during acute injury and regeneration.

## Results

### Met is required for normal muscle regeneration

To identify factors that directly regulate muscle stem cell behavior in vivo, we systematically assessed chemokine transcripts in regenerating muscle using published data sources (Hirata et al., 2003; Xiao et al., 2011; Bobadilla et al., 2014) and verified their expression using qPCR. A multitude of chemokines are rapidly and strongly induced after injury. In murine tibialis anterior muscle tissue, *Tnf* and *Hgf* transcripts were induced 10–500-fold with a time course that peaked 2–3 days after injury (Figure 1A and B, Figure 1—figure supplement 1, and Supplementary file 1). TNF $\alpha$  is known to orchestrate the inflammatory response and to participate in the communication between immune cells (Saclier et al., 2013a; Turner et al., 2014), and HGF is a proliferation and motility factor that can act as protective factor in tissue injury (Birchmeier et al., 2003; Nakamura and Mizuno, 2010). *Hgf* transcripts were produced at low levels by quiescent and activated muscle stem cells, demonstrating that other cell types but muscle stem cells produce *Hgf* in the regenerating muscle (Figure 1C and Supplementary file 1). This is in accord with previous data on *Hgf* expression obtained by microarray analysis (Liu et al., 2013; Latroche et al., 2017; see also Figure 1—figure supplement 1). The HGF receptor MET is expressed in adult muscle stem cells (Cornelison and Wold, 1997), and, in contrast to quiescent muscle stem cells, *Met* transcripts were upregulated when the cells were activated (Figure 1D).

To identify the role of HGF/MET during muscle repair, we introduced a loss-of-function mutation in *Met* in muscle stem cells using a constitutive *Pax7<sup>iresCre</sup>* allele (*Pax7<sup>iresCre</sup>;Met<sup>fllox/fllox</sup>* mice, named hereafter coMet; the genotype of the corresponding control mice used was *Pax7<sup>iresCre</sup>;Met<sup>+/+</sup>*). *Met* is known to control migration of myogenic progenitors during development (Bladt et al., 1995). The conditional mutation did not affect muscle progenitor migration because *Pax7* (and hence *Pax7<sup>iresCre</sup>*) starts only to be expressed in progenitors that have already reached their targets (Relaix et al., 2004). Therefore, the *Met* mutation in myogenic progenitors is introduced after migration is completed, from there on persisting throughout fetal and postnatal development. In the undamaged muscle, neither fiber diameter nor muscle stem cell numbers were changed in coMet mutant compared to control mice (Figures 2 and 3).

Upon injury of the *tibialis anterior* muscle using cardiotoxin, coMet mutant muscle stem cells were able to regenerate muscle fibers. However, at 7 days post injury (dpi) the diameter of the newly

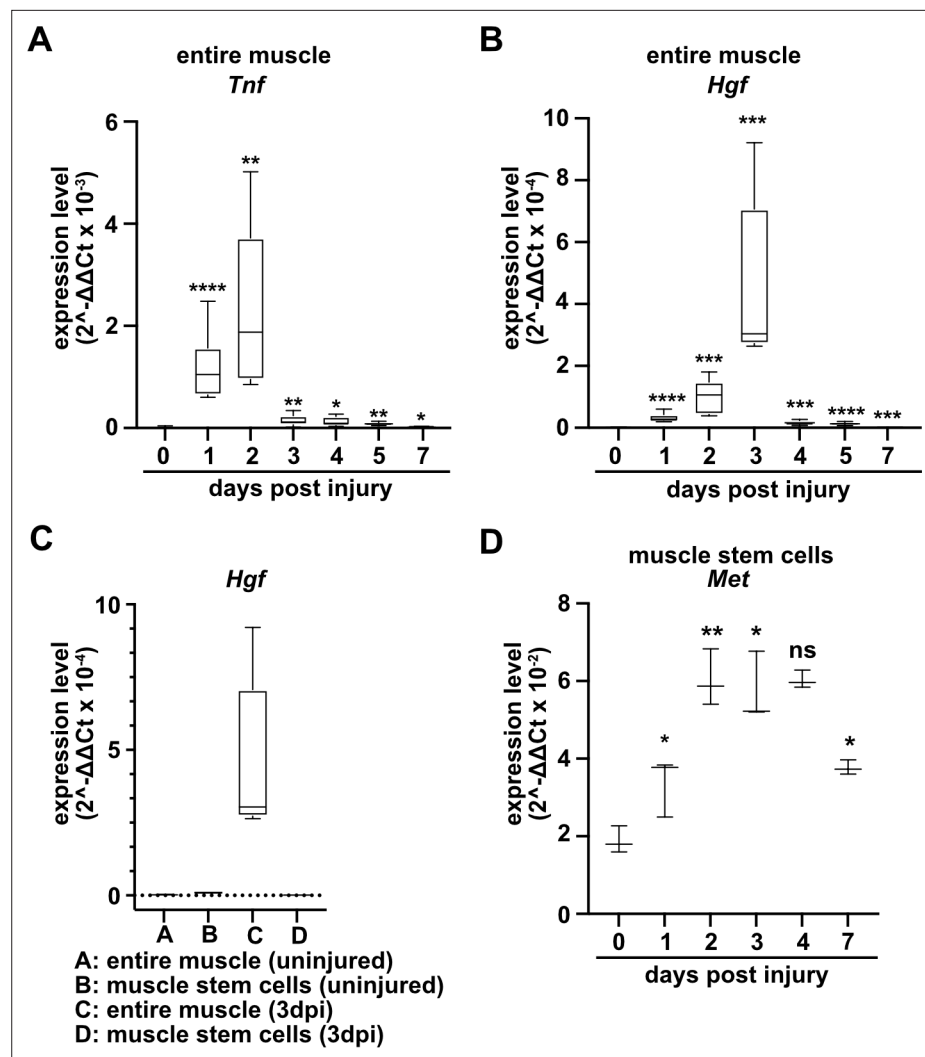


**Figure 1.** Expression of *Tnf*, *Hgf*, and *Met* during muscle regeneration. (A, B) Expression dynamics of *Tnf* (A) and *Hgf* (B) in uninjured and regenerating muscle tissue determined by qPCR. (C) Expression dynamics of *Hgf* in quiescent and activated muscle stem cells and in muscle tissue during muscle regeneration determined by qPCR. (D) Expression levels of *Met* in quiescent and activated muscle stem cells determined by qPCR. Boxplots represent interquartile range, and whiskers show min-to-max range.  $\beta$ -Actin expression was used for normalization in (A–D).

The online version of this article includes the following source data and figure supplement(s) for figure 1:

**Source data 1.** Quantification of *Tnf*, *Hgf* and *Met* expression represented in the diagrams shown in A–D.

**Figure supplement 1.** Expression levels of *Hgf* in quiescent (freshly isolated) and proliferating muscle stem cells at various time points defined by microarray analysis (Liu et al., 2013; Latroche et al., 2017).

regenerated fibers was smaller in *coMet* mutants than in control animals, but diameters largely equalized between control and *coMet* mutants and were no longer significantly different at 20 dpi (Figure 2A–D, quantified in E). Moreover, the number of PAX7<sup>+</sup> stem cells in the regenerated muscle of *coMet* mice was reduced by 68% at 7 dpi compared to control mice, and also this difference became less pronounced at 20 dpi (47% reduction in *coMet* mice; Figure 3A–F). Similar deficits were observed when *Met* was mutated in adult muscle stem cells using the tamoxifen-inducible *Pax7<sup>iiresCreERT2</sup>Gaka/+;Met<sup>fllox/fllox</sup>* allele (*Pax7<sup>iiresCreERT2</sup>Gaka/+;Met<sup>fllox/fllox</sup>* mice treated with tamoxifen, named hereafter Tx<sup>Gaka</sup>Met as controls, *Pax7<sup>iiresCreERT2</sup>Gaka/+;Met<sup>+/+</sup>* mice treated with tamoxifen were used). Thus, the diameter of new fibers was smaller at 7 dpi in Tx<sup>Gaka</sup>Met compared to control animals at 7 dpi, but at 20 dpi the difference in fiber diameters was no longer significant (Figure 2F–J). Moreover, the number of PAX7<sup>+</sup> stem cells in the regenerated muscle of Tx<sup>Gaka</sup>Met mice was reduced by 73% at 7 dpi compared to control, and also



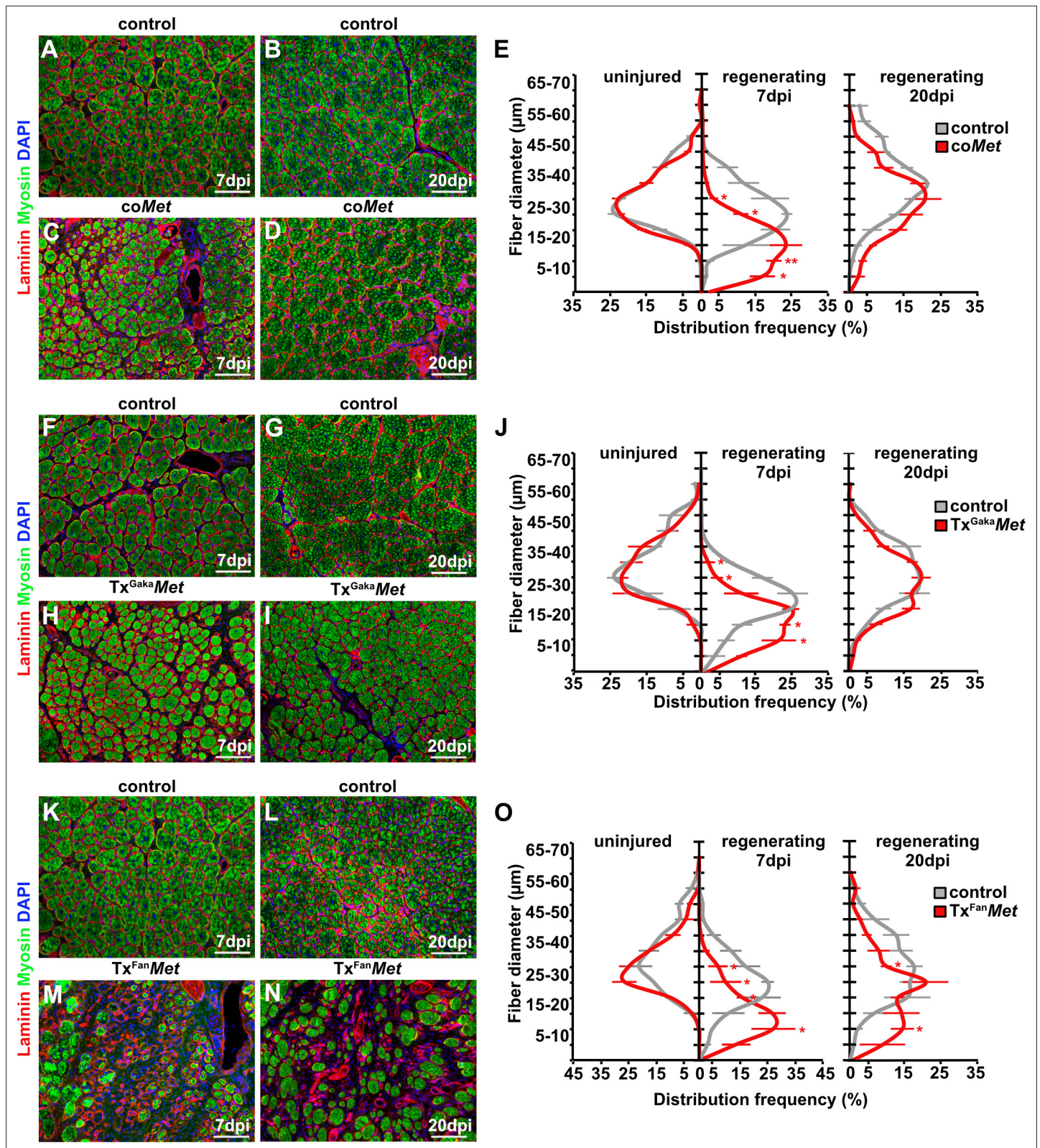


**Figure 2.** Mutation of *Met* impairs muscle regeneration. (A–D) Immunohistological analysis of regenerating (7 days post injury [dpi] and 20 dpi) muscle of control and coMet mutants using antibodies against laminin (red) and sarcomeric myosin (green). DAPI was used as a counterstain. (E) Distribution of Feret fiber diameters in uninjured and regenerating muscle (7 dpi and 20 dpi) of control mice and coMet mutants. (F–I) Immunohistological analysis of regenerating muscle of control and Tx<sup>Gaka</sup>Met mice using antibodies against laminin (red) and sarcomeric myosin (green). DAPI was used

Figure 2 continued on next page



Figure 2 continued

as a counterstain. (J) Distribution of Feret fiber diameters in uninjured and regenerating muscle (7 dpi and 20 dpi) of control and Tx<sup>Gaka</sup>Met mice. (K–N) Immunohistological analysis of regenerating (7 dpi and 20 dpi) muscle of control and Tx<sup>Fan</sup>Met mice using antibodies against laminin (red) and sarcomeric myosin (green). DAPI was used as a counterstain. (O) Distribution of Feret fiber diameters in uninjured and regenerating (7 dpi and 20 dpi) muscle of control and Tx<sup>Fan</sup>Met mice. Scale bars, 100 μm. In (A–E) control: Pax7<sup>iresCre/+;Met<sup>+/+</sup></sup>; coMet: Pax7<sup>iresCre/+;Met<sup>flox/flox</sup></sup>. In (F–J) control: Pax7<sup>iresCreERT2Gaka/+;Met<sup>+/+</sup></sup>; Tx<sup>Gaka</sup>Met: Pax7<sup>iresCreERT2Gaka/+;Met<sup>flox/flox</sup></sup>; In (K–O) control: Pax7<sup>CreERT2Fan/+;Met<sup>+/+</sup></sup>; Tx<sup>Fan</sup>Met: Pax7<sup>CreERT2Fan/+;Met<sup>flox/flox</sup></sup>. Animals in (F–O) were treated with tamoxifen.

The online version of this article includes the following source data for figure 2:

**Source data 1.** Quantification of fiber diameters represented in the diagrams shown in E, J and O.

this difference was less pronounced at 20 dpi (44% reduction in Tx<sup>Gaka</sup>Met mice) (**Figure 3G–L**). In summary, our data indicate that loss of *Met* in muscle stem cells results in a mild regeneration deficit. This is accompanied by a reduction of muscle stem cell numbers during early stages of regeneration, which is partly compensated for during late stages. Increased proliferation of the remaining stem cell pool might account for this (see below for a more detailed description of the mechanisms). A previous report had indicated that ablation of *Met* using a distinct tamoxifen-inducible Pax7<sup>CreERT2</sup> allele (Pax7<sup>CreERT2Fan</sup>) resulted in a much more severe muscle regeneration deficit (**Webster and Fan, 2013**). We used this Cre allele to mutate *Met* (Pax7<sup>CreERT2Fan/+;Met<sup>flox/flox</sup></sup> mice treated with tamoxifen, named hereafter Tx<sup>Fan</sup>Met animals; as controls, Pax7<sup>CreERT2Fan/+;Met<sup>+/+</sup></sup> mice treated with tamoxifen were used), and also detected a very severe muscle regeneration deficit at 7 dpi and 20 dpi compared to control animals at these stages of regeneration (**Figure 2K–O**). In particular, extracellular matrix remnants from injured skeletal muscle fibers (i.e., ghost fibers) were abundant at 7 dpi and 20 dpi. Notably, even in the uninjured muscle a 50 % reduction in the number of PAX7+ cells was observed in the Tx<sup>Fan</sup>Met animals compared to controls. This became more pronounced after injury when a 94 and 65% reduction in stem cell numbers was present at 7 dpi and 20 dpi, respectively, compared to the control animals at these stages of regeneration (**Figure 3M–R**). Different recombination efficacies did not account for these differences in phenotypes observed in coMet and Tx<sup>Gaka</sup>Met animals on one side, and Tx<sup>Fan</sup>Met animals on the other side (**Figure 3—figure supplement 1A–D**). We conclude that the muscle stem cell and regeneration deficits present in Tx<sup>Fan</sup>Met mutants are apparently not only due to the *Met* ablation. It should be noted that in the Pax7<sup>CreERT2Fan</sup> allele, the Pax7 coding sequence is disrupted by Cre, whereas the Pax7<sup>iresCreERT2Gaka</sup> and Pax7<sup>iresCre</sup> alleles do not interfere with the Pax7 coding sequence (**Keller et al., 2004; Lepper et al., 2009; Murphy et al., 2011**; see also **Figure 3—figure supplement 1E** for a cartoon of the different Cre alleles used). PAX7 levels are known to affect muscle stem cell behavior and their ability to regenerate the muscle (**von Maltzahn et al., 2013; Mademtoglou et al., 2018**). Thus, the absence of one functional Pax7 allele might contribute to the exacerbated muscle stem cell and regeneration phenotypes observed in Tx<sup>Fan</sup>Met animals.

## MET and CXCR4 signaling cooperates during muscle regeneration

The CXCR4 receptor is expressed in developing and adult muscle stem cells and mediates CXCL12 signals that stimulate their proliferation and migration (**Vasyutina et al., 2005; Odemis et al., 2007; Griffin et al., 2010**). *Cxcl12* is expressed by various cell types of the immune system. qPCR demonstrated that muscle tissue and PAX7+ cells expressed *Cxcl12* transcripts in both uninjured and regenerating muscle, and confirmed that *Cxcr4* transcripts were present in PAX7+ cells (**Figure 4A–C, Figure 4—figure supplement 1, and Supplementary file 1**). *Cxcr4* and *Met* are known to cooperate during muscle development (**Vasyutina et al., 2005**). We therefore tested whether this cooperativity was also observed in adult muscle stem cells and whether it would have an impact on muscle repair using *Cxcr4* and *Met* double mutant mice (Pax7<sup>iresCreERT2Gaka/+;Cxcr4<sup>flox/flox</sup>;Met<sup>flox/flox</sup></sup> mice treated with tamoxifen, hereafter called Tx<sup>Gaka</sup>Cxcr4;Met animals; Pax7<sup>iresCreERT2Gaka/+;Cxcr4<sup>+/+</sup>;Met<sup>+/+</sup></sup> treated with tamoxifen served as controls). Mutations of *Cxcr4* and *Met* in muscle stem cells did not obviously affect muscle formation or muscle stem cell numbers (**Figure 5, Figure 5—figure supplement 1**). However, Tx<sup>Gaka</sup>Cxcr4;Met double mutant mice at 7 dpi displayed a very severe regeneration deficit compared to control mice at 7 dpi. In particular, formation of myofibers was strongly impaired (**Figure 5A–E**). Further, the number of muscle stem cells detected at 7 dpi was decreased by 93 % as compared to control mice at 7 dpi (**Figure 5F–J**). The severe regeneration deficit was accompanied by widespread fibrosis, persisting macrophages,

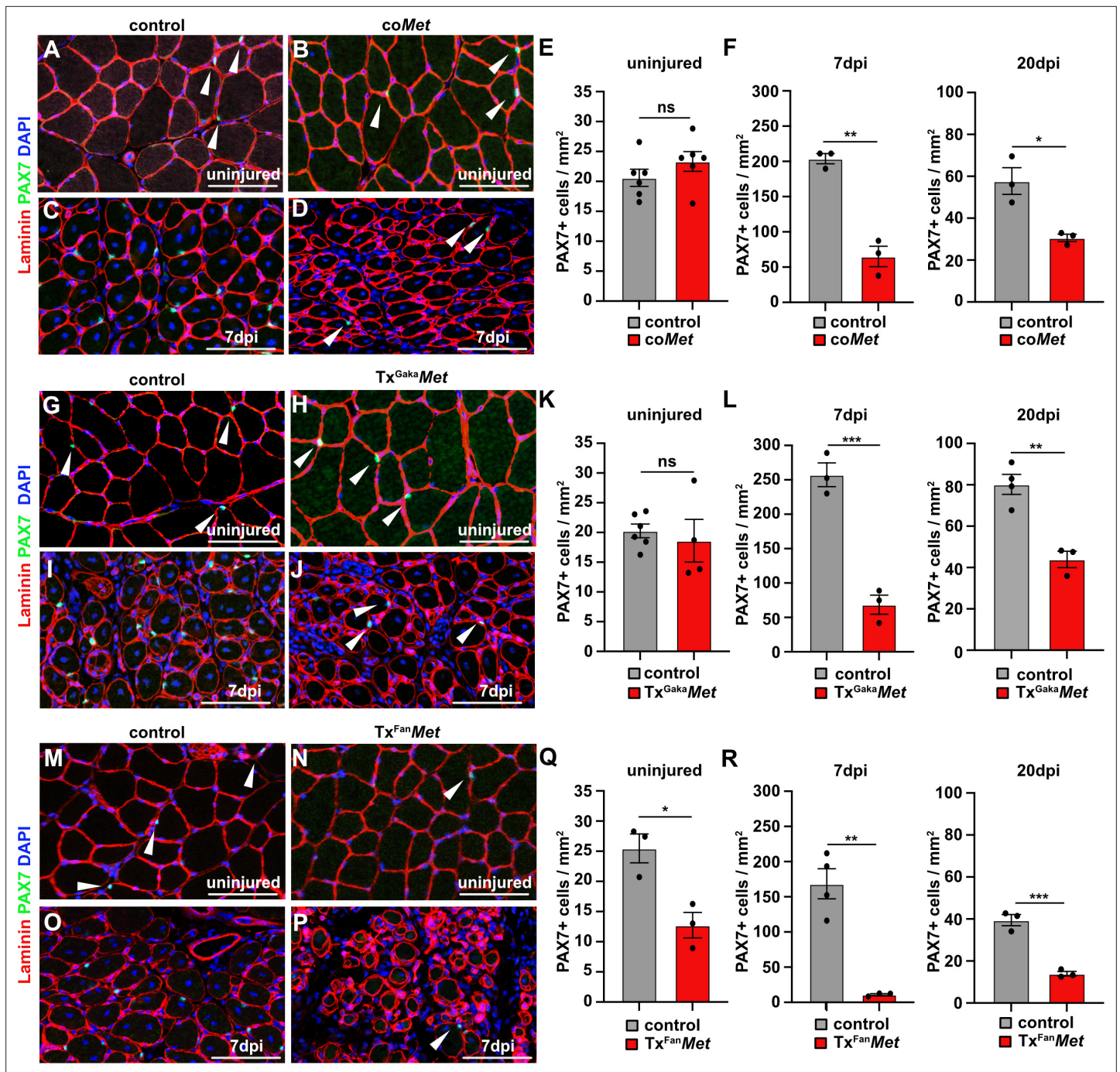


**Figure 3.** Mutation of *Met* reduces the muscle stem cell pool during regeneration. (A–D) Immunohistological analysis of uninjured and regenerating (7 days post injury [dpi]) muscle of control and *coMet* mice using antibodies against laminin (red) and PAX7 (green). DAPI was used as a counterstain. (E, F) Quantification of PAX7+ cells in uninjured and regenerating muscle from control and *coMet* mice. (G–J) Immunohistological analysis of uninjured and regenerating (7 dpi) muscle from control and *Tx<sup>Gaka</sup>Met* mice using antibodies against laminin (red) and Pax7 (green). DAPI was used as a counterstain. (K, L) Quantification of PAX7+ cells in uninjured and regenerating muscle of control and *Tx<sup>Gaka</sup>Met* mice. (M–P) Immunohistological analysis of uninjured and regenerating (7 dpi) muscle from control and *Tx<sup>Fan</sup>Met* mice using antibodies against laminin (red) and Pax7 (green). DAPI was used as a counterstain. (Q, R) Quantification of PAX7+ cells in uninjured and regenerating (7 dpi) muscle from control and *Tx<sup>Fan</sup>Met* mice. Arrowheads point to PAX7+ cells. Scale bars 100  $\mu$ m. In (A–F) control: *Pax7<sup>iResCre/+</sup>;Met<sup>+/+</sup>*; *coMet*: *Pax7<sup>iResCre/+</sup>;Met<sup>flx/flx</sup>*. In (G–L) control: *Pax7<sup>iResCreERT2Gaka/+</sup>;Met<sup>+/+</sup>*; *Tx<sup>Gaka</sup>Met*: *Pax7<sup>iResCreERT2Gaka/+</sup>;Met<sup>flx/flx</sup>*. In (M–R) control: *Pax7<sup>iResCreERT2Fan/+</sup>;Met<sup>+/+</sup>*; *Tx<sup>Fan</sup>Met*: *Pax7<sup>iResCreERT2Fan/+</sup>;Met<sup>flx/flx</sup>*. Animals in (G–R) were treated with tamoxifen.

The online version of this article includes the following source data and figure supplement(s) for figure 3:

**Source data 1.** Quantification of PAX7+ cells represented in the diagrams shown in E, F, K, L, Q and R (Figure 3).

**Figure supplement 1.** Recombination efficiency and schematic drawing of the different *Pax7*Cre alleles.

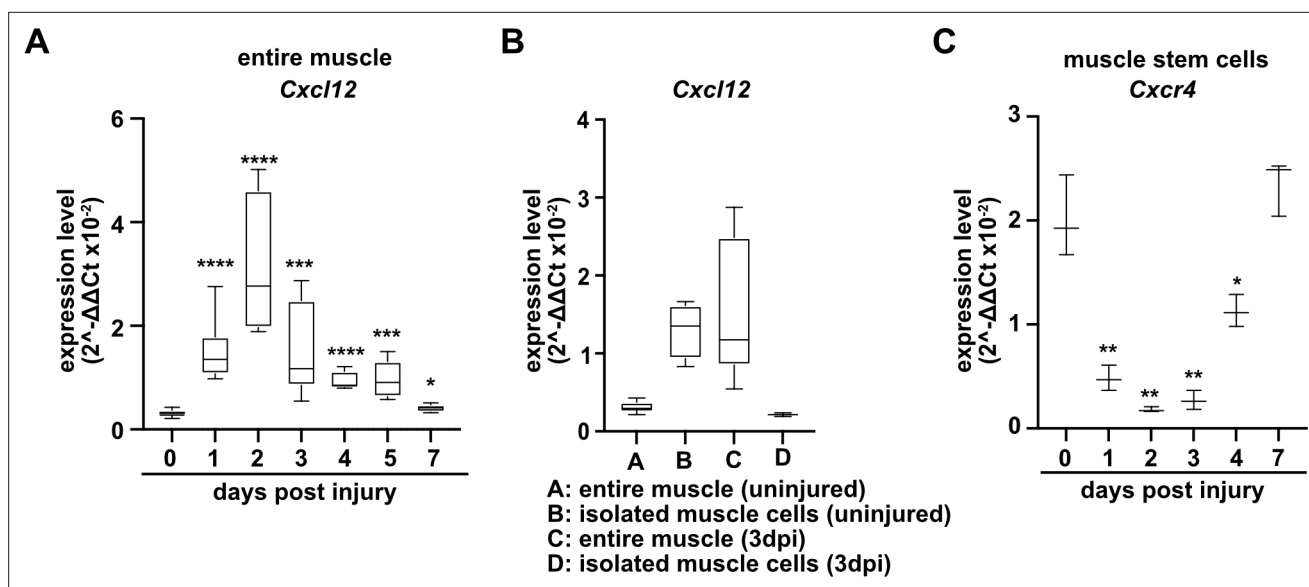


**Figure 4.** Expression of *Cxcl12* and *Cxcr4* during regeneration. (A) Expression dynamics of *Cxcl12* in uninjured and regenerating muscle tissue determined by qPCR. (B) Expression levels of *Cxcl12* in quiescent and activated muscle stem cells and in muscle tissue during muscle regeneration determined by qPCR. (C) Expression levels of *Cxcr4* in quiescent and activated muscle stem cells determined by qPCR. Boxplots represent interquartile range, whiskers show min-to-max range.  $\beta$ -Actin expression was used for normalization in (A–C).

The online version of this article includes the following source data and figure supplement(s) for figure 4:

**Source data 1.** Quantification of *Cxcl12* and *Cxcr4* expression represented in the diagrams shown in A–C.

**Figure supplement 1.** Expression levels of *Cxcl12* in quiescent (freshly isolated) and proliferating muscle stem cells at various time points defined by microarray analysis (Liu et al., 2013; Latroche et al., 2017).

and prolonged inflammation (Figure 5—figure supplement 2). In contrast, the single *Cxcr4* mutation in muscle stem cells (*Pax7<sup>iresCreERT2Gaka/+</sup>;Cxcr4<sup>fllox/fllox</sup>* treated with tamoxifen, hereafter named Tx<sup>Gaka</sup>*Cxcr4*; *Pax7<sup>iresCreERT2Gaka/+</sup>;Cxcr4<sup>+/+</sup>* mice treated with tamoxifen served as controls) did neither affect the number of muscle stem cells in regeneration, the diameter of newly formed fibers, nor did it cause prolonged inflammation or fibrosis (Figure 5, Figure 5—figure supplement 1, and Figure 5—figure supplement 2). We conclude that loss of muscle stem cells and deficits in muscle repair are augmented if both *Cxcr4* and *Met* are lacking.

### Muscle stem cells deficient for *Met* and *Cxcr4* are susceptible to apoptosis

We next assessed the mechanisms by which the *Cxcr4* and *Met* mutations affect muscle stem cell maintenance in the injured muscle. We observed a pronounced increase in apoptosis of PAX7+ cells at 4 dpi in the double mutants and a severe decrease in the number of PAX7+ muscle stem cells (Figure 6). A less pronounced enhancement of apoptosis of muscle stem cells was observed in Tx<sup>Gaka</sup>*Met* single mutants, whereas the Tx<sup>Gaka</sup>*Cxcr4* single mutation did not significantly impair survival as compared to control animals (Figure 6). Thus, the signals provided by CXCR4 and MET protect muscle stem cells from apoptosis in the acutely injured muscle.

CXCR4 and MET signals stimulate muscle stem cell proliferation in vitro (Allen et al., 1995; Cornelison, 2008). However, in the regenerating muscle in vivo, ablation of *Cxcr4* and *Met* in muscle stem cells did not impair their proliferation. On the contrary, EdU incorporation showed that proliferation of muscle stem cells increased in the Tx<sup>Gaka</sup>*Cxcr4*;*Met* double and Tx<sup>Gaka</sup>*Met* single mutants (Figure 6—figure supplement 1), possibly due to compensatory mechanisms. Moreover, in Tx<sup>Gaka</sup>*Cxcr4*;*Met* double and Tx<sup>Gaka</sup>*Met* single mutants, the ratio of MyoG+/Pax7+ cells was slightly increased, indicating that differentiation was mildly enhanced (Figure 6—figure supplement 2). We conclude that CXCR4 and MET signals cooperate to convey powerful cyto-protective functions.



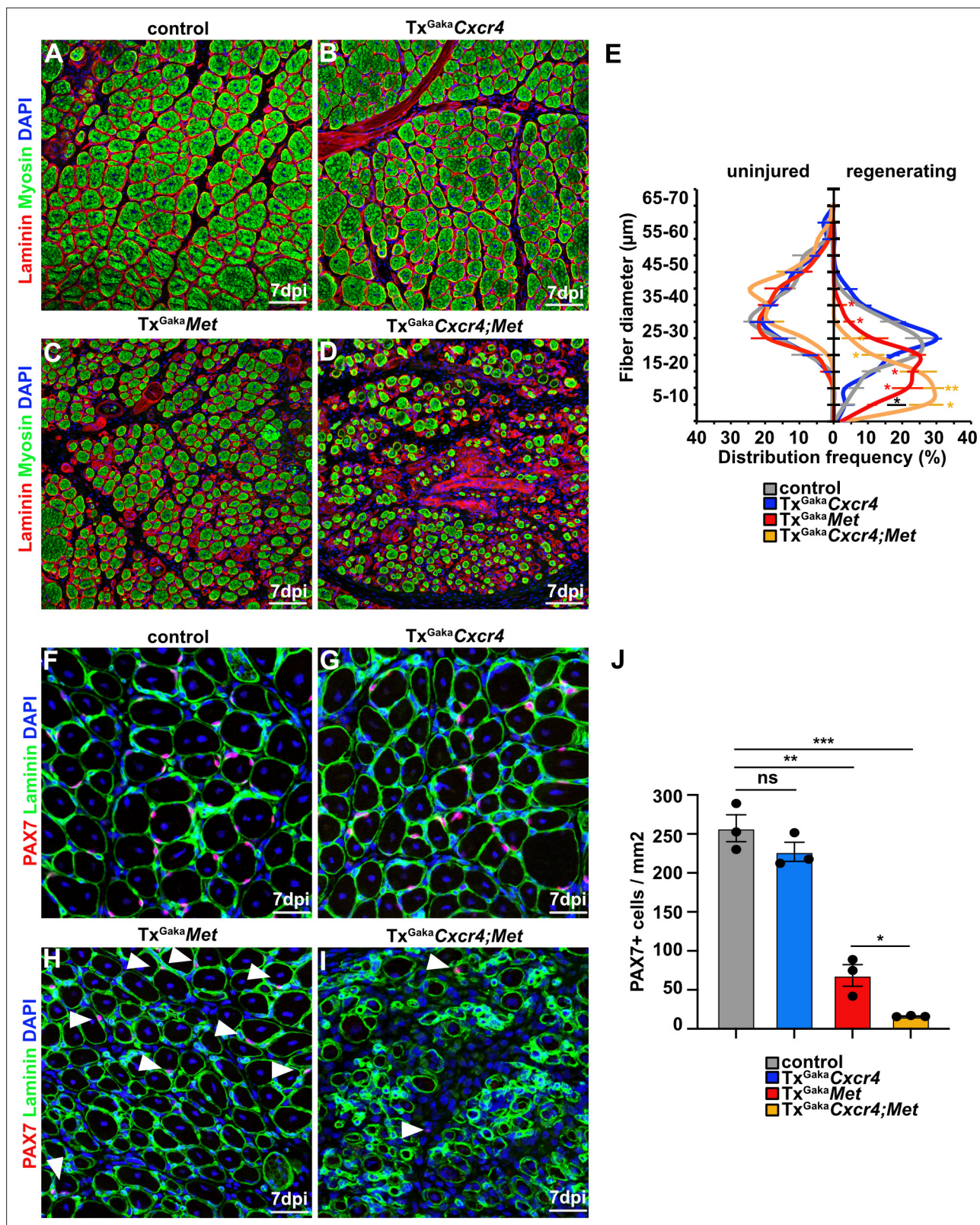


**Figure 5.** *Cxcr4* and *Met* cooperate during muscle regeneration. (A–D) Immunohistological analysis of regenerating (7 days post injury [dpi]) muscle of control, Tx<sup>Gaka</sup>Cxcr4, Tx<sup>Gaka</sup>Met, and Tx<sup>Gaka</sup>Cxcr4;Met mice using antibodies against laminin (red) and sarcomeric myosin (green). DAPI was used as a counterstain. Control and mutant animals had been treated with tamoxifen. (E) Distribution of Ferret fiber diameters in uninjured and regenerating (7 dpi) muscle of control, Tx<sup>Gaka</sup>Cxcr4, Tx<sup>Gaka</sup>Met, and Tx<sup>Gaka</sup>Cxcr4;Met mice. (F–I) Immunohistological analysis of regenerating (7 dpi) muscle of control

Figure 5 continued on next page

Figure 5 continued

animals,  $Tx^{Gaka}Cxcr4$ ,  $Tx^{Gaka}Met$ , and  $Tx^{Gaka}Cxcr4;Met$  mutants using antibodies against laminin (green) and Pax7 (red). DAPI was used as a counterstain. Arrowheads in (H, I) point to PAX7+ cells. (J) Quantification of PAX7+ cells in regenerating muscle of control,  $Tx^{Gaka}Cxcr4$  and  $Tx^{Gaka}Met$  mice, and  $Tx^{Gaka}Cxcr4;Met$  double mutants. Scale bars, 50  $\mu m$  (A–D), 30  $\mu m$  (F–I). Control:  $Pax7^{iresCreERT2Gaka/+}$ ;  $Tx^{Gaka}Cxcr4$ :  $Pax7^{iresCreERT2Gaka/+};Cxcr4^{fllox/fllox}$ ;  $Tx^{Gaka}Met$ :  $Pax7^{iresCreERT2Gaka/+};Met^{fllox/fllox}$ ;  $Tx^{Gaka}Cxcr4;Met$ :  $Pax7^{iresCreERT2Gaka/+};Cxcr4^{fllox/fllox};Met^{fllox/fllox}$ . All animals were treated with tamoxifen.

The online version of this article includes the following source data and figure supplement(s) for figure 5:

**Source data 1.** Quantification of fiber diameters, PAX7+ cells and fibrotic area represented in the diagrams shown in E, J (Figure 5), E (Figure 5—figure supplement 1) and E, F (Figure 5—figure supplement 2).

**Figure supplement 1.** Mutations of Cxcr4 and Met in muscle stem cells did not affect muscle stem cell numbers.

**Figure supplement 2.** Increased fibrosis in the regenerating muscle of Met and Cxcr4;Met mutants.

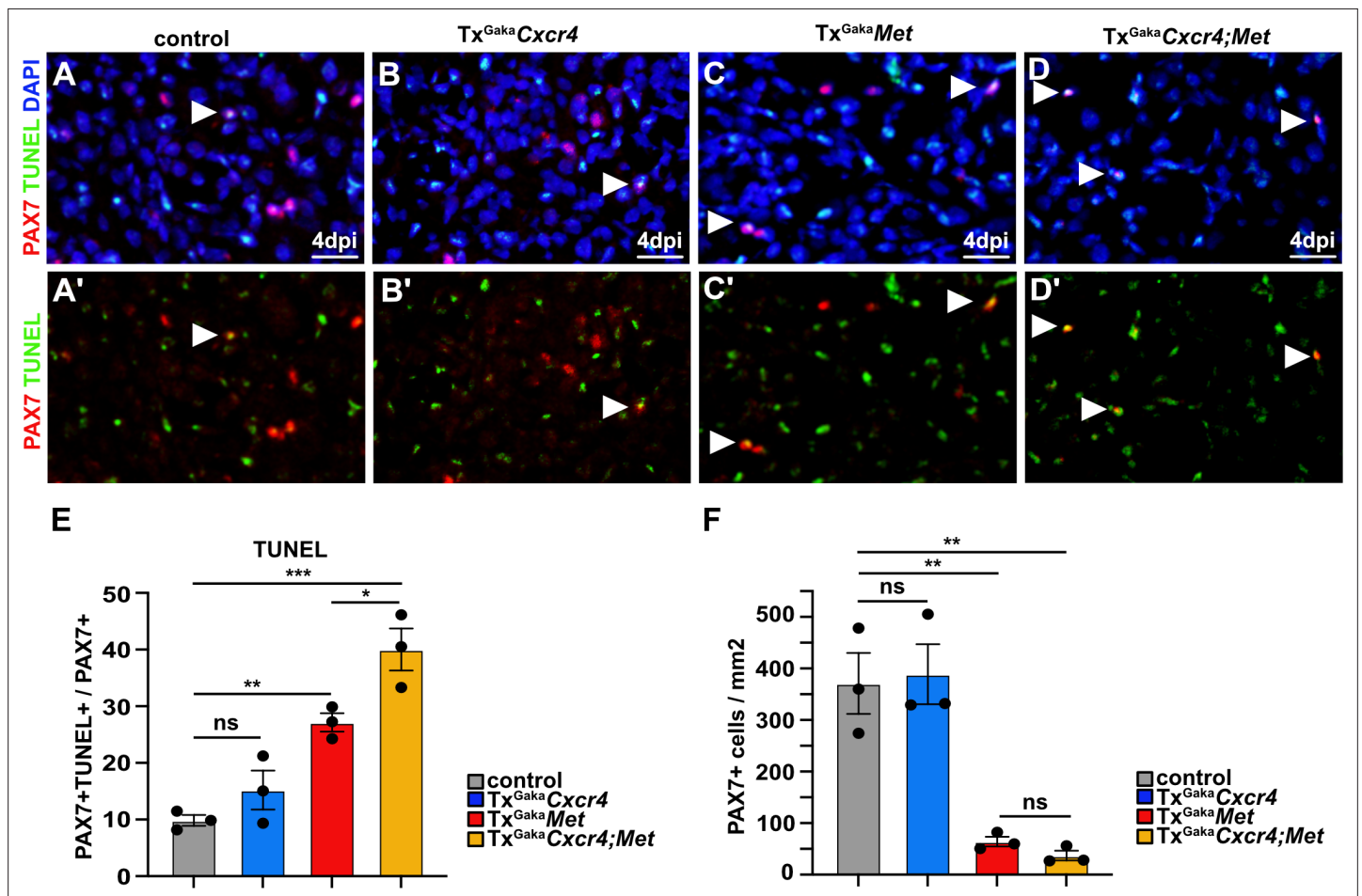


**Figure 6.** *Cxcr4;Met* mutant muscle stem cells undergo apoptosis after acute injury. (A–D, A'–D') Immunohistological analysis of apoptotic cells. PAX7 antibody staining (red) was combined with TUNEL assay (green) to identify apoptotic muscle stem cells in injured muscle of control,  $Tx^{Gaka}Cxcr4$ ,  $Tx^{Gaka}Met$ , and  $Tx^{Gaka}Cxcr4;Met$  mice at 4 days post injury (dpi). DAPI was used as a counterstain in (A–D). Arrowheads point to TUNEL+ PAX7+ cells. (E) Quantification of PAX7+ TUNEL+ cells in regenerating muscle of control,  $Tx^{Gaka}Cxcr4$ ,  $Tx^{Gaka}Met$ , and  $Tx^{Gaka}Cxcr4;Met$  mutants. (F) Quantification of PAX7+ cells in regenerating muscle of control,  $Tx^{Gaka}Cxcr4$ ,  $Tx^{Gaka}Met$ , and  $Tx^{Gaka}Cxcr4;Met$  mice. Scale bars, 20  $\mu m$ . Control:  $Pax7^{iresCreERT2Gaka/+}$ ;  $Tx^{Gaka}Cxcr4$ :  $Pax7^{iresCreERT2Gaka/+};Cxcr4^{fllox/fllox}$ ;  $Tx^{Gaka}Met$ :  $Pax7^{iresCreERT2Gaka/+};Met^{fllox/fllox}$ ;  $Tx^{Gaka}Cxcr4;Met$ :  $Pax7^{iresCreERT2Gaka/+};Cxcr4^{fllox/fllox};Met^{fllox/fllox}$ . All animals were treated with tamoxifen.

The online version of this article includes the following source data and figure supplement(s) for figure 6:

**Source data 1.** Quantification of PAX7+TUNEL+ and PAX7+ cells represented in the diagrams shown in E and F (Figure 6).

**Figure supplement 1.** Enhanced proliferation of PAX7+ cells in *Cxcr4;Met* mutants during regeneration.

**Figure supplement 2.** Differentiation is mildly enhanced in *Met* and *Cxcr4;Met* mutants during regeneration.



## MET and CXCR4 signaling protects muscle cells from TNF $\alpha$ -induced apoptosis

We next aimed to identify the factor that induces apoptosis of *Met*; *Cxcr4* mutant muscle stem cells in the injured muscle. The pro-inflammatory cytokine TNF $\alpha$  is induced at the early stages of muscle regeneration and has pro- as well as anti-apoptotic effects on many cell types (*Darnay and Aggarwal, 1999; Malka et al., 2000; Collins and Grounds, 2001; Zador et al., 2001; Warren et al., 2002; Aggarwal, 2003*). We thus asked whether TNF $\alpha$  production might be responsible for the observed cell death. If freshly isolated muscle stem cells were cultured in media containing 2 % horse serum, TNF $\alpha$  induced apoptosis (**Figure 7A and B**). This TNF $\alpha$ -induced cell death of cultured cells was rescued by the addition of HGF and CXCL12, or by the addition of 10 % fetal calf serum. No cooperative effect of HGF and CXCL12 was observed in this cell culture setting (**Figure 7C and D**).

Finally, using neutralizing antibodies against TNF $\alpha$ , we tested whether the loss of muscle stem cells in the absence of MET and CXCL12 signaling during regeneration *in vivo* was caused by TNF $\alpha$ . The efficacy TNF $\alpha$  antibodies was verified in a cell culture experiment (**Figure 7—figure supplement 1**). We observed a pronounced rescue of PAX7+ cells in the regenerating muscle of *Tx<sup>Gaka</sup>Met* and *Tx<sup>Gaka</sup>Cxcr4;Met* mutant mice after injection of TNF $\alpha$  neutralizing antibodies (**Figure 7E–P**). Taken together, these data demonstrate that MET and CXCR4 signaling cooperate *in vivo* to protect muscle stem cells from TNF $\alpha$ -induced apoptosis in the inflammatory environment encountered after injury.

## Discussion

Muscle injury results in an acute inflammatory response causing the recruitment of macrophages and neutrophils. These cells remove cellular debris at the site of injury and provide signals that are beneficial for muscle repair. In addition, they release a multitude of chemokines, as well as reactive oxygen species and enzymes needed to degrade the debris, thereby creating a hostile environment that muscle stem cells have to withstand in order to regenerate the muscle and self-renew (*Tidball, 2005; Chazaud et al., 2009; Saclier et al., 2013b; Londhe and Guttridge, 2015; Tidball, 2017*). Our analysis of the *in vivo* function of MET and CXCR4 demonstrates an important cooperative role in muscle repair that protects stem cells against the adverse environment created by the acute inflammatory response.

Previous studies had shown that HGF can elicit muscle stem cell proliferation in culture and that CXCL12 has mitogenic activity on myogenic C2C12 cells (*Allen et al., 1995; Gal-Levi et al., 1998; Odemis et al., 2007*). Further, injection of HGF into the intact muscle activates muscle stem cells (*Tatsumi et al., 1998*), and ablation of *Met* in muscle stem cells interferes with entry into *G<sub>al</sub><sup>ert</sup>*, a 'alerted' state of quiescence observed in muscle stem cells after injury of the contralateral muscle or of other unrelated organs (*Rodgers et al., 2014*). HGF/MET signaling also affects additional aspects of muscle stem cell biology. In particular, HGF suppresses differentiation of cultured myogenic cell lines and of primary muscle stem cells (*Gal-Levi et al., 1998; Siegel et al., 2009*). Thus, HGF had been implicated in multiple aspects of muscle stem cell behaviors, but its role as cyto-protective factor had not been addressed.

Interestingly, cyto-protective functions of HGF/MET were reported in several cell types and injury models, indicating that HGF might be part of a general defensive mechanism in response to tissue damage. In particular, ectopic application of HGF prior to or shortly after an insult protects cells in the liver, kidney, and heart from damage (*Ueda et al., 1999; Zhou et al., 2013; Matsumoto et al., 2014; Pang et al., 2018*). Moreover, after injury to the liver, kidney, heart, or skeletal muscle, increased HGF expression can be observed in the damaged organs, and plasma levels of HGF rise quickly after injury (*Michalopoulos and DeFrances, 1997; Nakamura et al., 2000; Matsumoto and Nakamura, 2001*). It was proposed that release from extracellular matrix might account for the fast rise in HGF plasma levels (*Shimomura et al., 1995; Tatsumi et al., 1998*). In addition, various cytokines, among them interleukin-1 and interleukin-6, activate HGF transcription, which might account for the increased HGF transcripts observed after tissue damage (*Birchmeier et al., 2003*). We demonstrate here that loss of *Met* impairs the resistance of muscle stem cells against acute inflammation. Moreover, *in vivo* the additional loss of *Cxcr4* exacerbated the deficits observed after loss of *Met*. The cooperative effect that we detected here *in vivo* is reflected by the fact that both receptors, *Met* and *Cxcr4*, use in part overlapping downstream signaling cascades but also activate distinct signaling molecules. Tyrosine



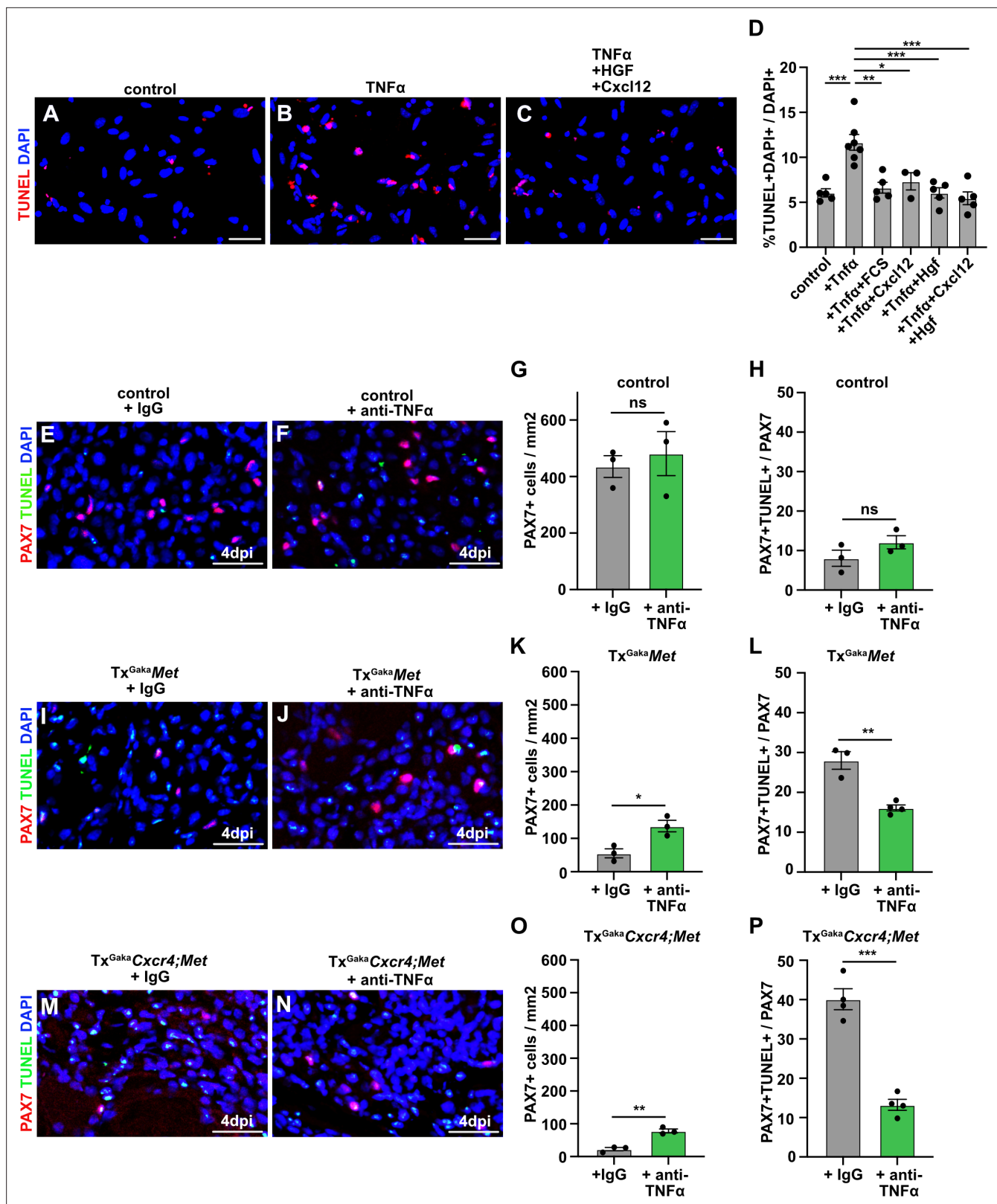


**Figure 7.** CXCL12 and HGF protect muscle cells from TNF $\alpha$ -induced cell death. (A–C) Primary muscle stem cells were isolated and cultured for 3 hr in the presence of TNF $\alpha$  plus/minus HGF and Cxcl12. Apoptotic cells were identified by TUNEL staining. (D) Quantification of TUNEL+ cells present in such cultures. (E, F) Immunohistological analysis of muscle stem cells (PAX7+, red) and apoptotic cells (TUNEL staining, green) in injured muscle (4 days post injury [dpi]) of control mice treated with TNF $\alpha$  neutralizing antibodies or control IgG 2 hr before acute injury. DAPI was used as a

Figure 7 continued on next page

Figure 7 continued

counterstain. **(G)** Quantification of PAX7+ cells in regenerating muscle (4 dpi) of control mice treated with TNF $\alpha$  neutralizing antibodies or control IgG. **(H)** Quantification of PAX7+ TUNEL+ cells in regenerating muscle (4 dpi) of control mice treated with TNF $\alpha$  neutralizing antibodies or control IgG. **(I, J)** Immunohistological analysis of muscle stem cells (PAX7+, red) and apoptotic cells (TUNEL staining, green) in injured muscle (4 dpi) of Tx<sup>Gaka</sup>Met mutants treated with TNF $\alpha$  neutralizing antibodies or control IgG 2 hr before acute injury. DAPI was used as a counterstain. **(K)** Quantification of PAX7+ cells in regenerating (4 dpi) muscle of Tx<sup>Gaka</sup>Met mice treated with TNF $\alpha$  neutralizing antibodies or control IgG. **(L)** Quantification of PAX7+ TUNEL+ cells in regenerating muscle from Tx<sup>Gaka</sup>Met mice treated with TNF $\alpha$  neutralizing antibodies or control IgG. **(M, N)** Immunohistological analysis of muscle stem cells (PAX7+, red) and apoptotic cells (TUNEL staining, green) in injured muscle (4 dpi) of Tx<sup>Gaka</sup>Cxcr4;Met mutants treated with TNF $\alpha$  neutralizing antibodies or control IgG 2 hr before acute injury. DAPI was used as a counterstain. **(O)** Quantification of PAX7+ cells in regenerating muscle (4 dpi) of Tx<sup>Gaka</sup>Cxcr4;Met mice treated with TNF $\alpha$  neutralizing antibodies or control IgG. **(P)** Quantification of PAX7+ TUNEL+ cells in regenerating muscle (4 dpi) of Tx<sup>Gaka</sup>Cxcr4;Met mice treated with TNF $\alpha$  neutralizing antibodies or control IgG. Scale bars, 20  $\mu$ m. Control: Pax7<sup>iresCreERT2Gaka/+</sup>; Met<sup>fllox/flox</sup>; Tx<sup>Gaka</sup>Met: Pax7<sup>iresCreERT2Gaka/+</sup>; Met<sup>fllox/flox</sup>; Tx<sup>Gaka</sup>Cxcr4;Met: Pax7<sup>iresCreERT2Gaka/+</sup>; Cxcr4<sup>fllox/flox</sup>; Met<sup>fllox/flox</sup>. All animals were treated with tamoxifen.

The online version of this article includes the following source data and figure supplement(s) for figure 7:

**Source data 1.** Quantification of TUNEL+, PAX7+ and PAX7+TUNEL+ cells represented in the diagrams shown in D, G, H, K, L, O and P (**Figure 7**).

**Figure supplement 1.** Neutralizing capacity of TNF $\alpha$  antibody used in **Figure 7**.

phosphorylation of MET results in the activation of various signaling events that regulate cell motility, proliferation, and survival; among them RAS/MAPK, PI3-kinase/AKT, PLC $\gamma$ /PKC, RAC/CDC42, and CRK (Birchmeier et al., 2003; Gentile et al., 2008). CXCR4 uses G-proteins to transmit signals into the cytoplasm, which involves activation of second messenger-regulated serine/threonine kinases or ion channels. However, CXCR4 also activates RAS/MAPK, PI3-kinase/AKT, and CRK signaling, which is particularly well documented in cancer cells (Teicher and Fricker, 2010). Among these cascades, PI3-kinase/AKT is well known to act anti-apoptotically, and MAPK/ERK signals can counteract the apoptotic activity of TNF $\alpha$  (Tran et al., 2001; Franke et al., 2003).

TNF $\alpha$  is one of many pro-inflammatory cytokines that are rapidly induced upon acute muscle injury, and TNF $\alpha$  is highly expressed by pro-inflammatory macrophages. The primary role of TNF $\alpha$  is to regulate immune cells, but it also affects the proliferation and differentiation of cultured muscle cells (Wallach et al., 1999; Li, 2003; Luo et al., 2005; Palacios et al., 2010). Mice lacking TNF $\alpha$  receptors p55 and p75 show that TNF $\alpha$  does not play an essential role in muscle regeneration, indicating that this cytokine seems to act redundantly with other factors (Collins and Grounds, 2001). However, systemic injection of TNF $\alpha$  neutralizing antibodies protected dystrophic skeletal muscle of mdx mice from necrosis and increased the number of PAX7+ cells (Palacios et al., 2010). This indicates that TNF $\alpha$  exacerbates muscle fiber damage and, in addition, impairs muscle stem cell maintenance in dystrophic muscle. Our analysis indicates that TNF $\alpha$  signals are also damaging for muscle stem cells during acute inflammation after injury, but that endogenous HGF and CXCL12 may counteract this. Effects of TNF $\alpha$  are modulated by other signals, and particularly MAPK/ERK activity can override the apoptotic TNF $\alpha$  signal (Tran et al., 2001; Aggarwal, 2003; Wada and Penninger, 2004; Lu and Xu, 2006; Lau et al., 2011). Acute skeletal muscle injury resulting in inflammation is a common clinical condition caused by trauma, severe contraction, chemicals, myotoxins, and ischemia. Similarly, acute inflammation is observed in muscle diseases like dystrophy (Kharraz et al., 2014; Tidball et al., 2018). Our genetic experiments indicate that HGF/MET and CXCL12/CXCR4 signaling protects muscle stem cells against the noxious environment generated by the inflammatory response. Exogenous HGF was previously tested in muscle injury and increased the numbers of activated muscle stem cells, but did not enhance fiber growth (Miller et al., 2000). Thus, in healthy muscle, endogenous factors, among them HGF, suffice to ensure appropriate regeneration. Nevertheless, in muscle disease where repair mechanisms fail, enhanced cyto-protection of muscle stem cells appears to be beneficial (Palacios et al., 2010). Whether HGF/MET and CXCL12/CXCR4 signaling protects against TNF $\alpha$ -induced damage in such disease settings will need further investigation.

## Materials and methods

### Key resources table

Reagent type (species) or resource	Designation	Source or reference	Identifiers	Additional information
Antibody	Guinea pig polyclonal anti-PAX7	Our lab	PMID:22940113	1:2500

*Continued on next page*

Reagent type (species) or resource	Designation	Source or reference	Identifiers	Additional information
Antibody	Rabbit polyclonal anti-Laminin	Sigma-Aldrich	L9393 RRID:AB_477163	1:500
Antibody	Goat polyclonal anti-CollagenIV	Millipore	AB769 RRID:AB_92262	1:500
Antibody	Mouse monoclonal anti-sarcomeric myosin	DSHB	MF20 RRID:AB_2147781	1:10
Antibody	Rabbit polyclonal anti-Myogenin	Abcam	ab124800 RRID:AB_10971849	1:1000
Antibody	Mouse monoclonal anti-F4/80	Abcam	ab6640 RRID:AB_1140040	1:100
Antibody	Rabbit polyclonal anti-fibronectin	Sigma-Aldrich	F7387 RRID:AB_476988	1:500
Antibody	Cy2, Cy3, Cy5 conjugated antibodies	Dianova		1:500
Commercial assay or kit	In Situ Cell Death Detection Kit	Roche	12156792910	
Commercial assay or kit	EdU	basedlick GmbH	BCK-EdU647	
Commercial Assay or kit	qPCR SYBR Green Mix	Thermo Fisher	AB1158B	
Sequence-based reagent	ATCCACGATGTTTCATGAGAG	Eurofins	N/A	qPCR HGF (forward primer)
Sequence-based reagent	GCTGACTGCATTTCTCATTC	Eurofins	N/A	qPCR HGF (reverse primer)
Sequence-based reagent	CACAGAAAGCATGATCCGCGACGT	Eurofins	N/A	qPCR TNF (forward primer)
Sequence-based reagent	CGGCAGAGAGGAGGTTGACTTTCT	Eurofins	N/A	qPCR TNF (reverse primer)
Sequence-based reagent	CAGAGCCAACGTCAAGCA	Eurofins	N/A	qPCR Cxcl12 (forward primer)
Sequence-based reagent	AGGTACTCTTGATCCAC	Eurofins	N/A	qPCR Cxcl12 (reverse primer)
Sequence-based reagent	CATTTTGCTGTGTCTATCATG	Eurofins	N/A	qPCR Met (forward primer)
Sequence-based reagent	ACTCCTCAGGCAGATTCCC	Eurofins	N/A	qPCR Met (reverse primer)
Sequence-based reagent	TCAGTGGCTGACCTCCTCTT	Eurofins	N/A	qPCR CXCR4 (forward primer)
Sequence-based reagent	CTTGGCCTTTGACTGTTGGT	Eurofins	N/A	qPCR CXCR4 (reverse primer)
Sequence-based reagent	CATTTTGCTGTGTCTATCATG	Eurofins	N/A	qPCR Met Exon 17 (forward primer)
Sequence-based reagent	ACTCCTCAGGCAGATTCCC	Eurofins	N/A	qPCR Met Exon 18 (reverse primer)
Sequence-based reagent	CTTGCCAGAGACATGTACGAT	Eurofins	N/A	qPCR Met Exon 20 (forward primer)
Sequence-based reagent	AGGAGCACACCAAAGGACCA	Eurofins	N/A	qPCR Met Exon 21 (reverse primer)
Sequence-based reagent	CCAGTTGGTAACAATGCCATGT	Eurofins	N/A	qPCR $\beta$ -actin (forward primer)
Sequence-based reagent	GGCTGTATCCCCTCCATCG	Eurofins	N/A	qPCR $\beta$ -actin (reverse primer)
Sequence-based reagent	ACTAGGCTCCACTCTGCCTTC	Eurofins	PMID:19554048	Genotyping PCR-Primer 1 Pax7CreERT2Fan
Sequence-based reagent	GCAGATGTAGGGACATTCCAGTG	Eurofins	PMID:19554048	Genotyping PCR-Primer 2 Pax7CreERT2Fan
Sequence-based reagent	GCTGCTGTTGATTACCTGGC	Eurofins	PMID:21828091	Genotyping PCR-Primer 1 Pax7CreERT2GaKa
Sequence-based reagent	CTGCACTGAGACAGGACCG	Eurofins	PMID:21828091	Genotyping PCR-Primer 2 Pax7CreERT2GaKa



Reagent type (species) or resource	Designation	Source or reference	Identifiers	Additional information
Sequence-based reagent	GCTGCTGTTGATTACCTGGC	Eurofins	PMID:21828091	Genotyping PCR-Primer 1 Pax7CreERT2GaKa
Sequence-based reagent	GCTCTGGATACACCTGAGTCT	Eurofins	PMID:15520281	Genotyping PCR-Primer 1 Pax7-IREScre
Sequence-based reagent	GGATAGTGAAACAGGGGCAA	Eurofins	PMID:15520281	Genotyping PCR-Primer 2 Pax7-IREScre
Sequence-based reagent	TCGGCCTTCTTCTAGTTCTGCTC	Eurofins	PMID:15520281	Genotyping PCR-Primer 3 Pax7-IREScre
Sequence-based reagent	CCACCCAGGACAGTGTGACTCTAA	Eurofins	PMID:15520246	Genotyping PCR-Primer 1 Cxcr4 flox
Sequence-based reagent	GATGGGATTCTGTATGAGGATTAGC	Eurofins	PMID:15520246	Genotyping PCR-Primer 2 Cxcr4 flox
Sequence-based reagent	CCAAGTGTCTGACGGCTGTG	Eurofins	N/A	Genotyping PCR-Primer 1 Met flox
Sequence-based reagent	AGCCTAGTGGAAATTCTCTGTAAG	Eurofins	N/A	Genotyping PCR-Primer 2 Met flox

## RNA isolation and qPCR

RNA from the entire muscle and from FACS-isolated muscle stem cells was extracted using TRIzol reagent (15596026, Thermo Fisher Scientific) following the manufacturer's instructions. qPCR was performed using SYBR green master mix (4309155, Thermo Fisher Scientific) as described previously (Bröhl *et al.*, 2012). PCR primers are listed in Key resources table.  $\beta$ -Actin was used for normalization.

## Immunohistochemistry

Immunohistochemistry was performed on 12  $\mu$ m cryo-sections of muscle biopsy samples fixed in Zamboni's fixative for 20 min as described previously (Bröhl *et al.*, 2012). For staining of Pax7, sections were incubated in Antigen Unmasking Solution buffer (H-3300, Vector Laboratories) for 20 min at 80 °C. Primary and secondary antibodies used are listed in Key resources table. Primary antibodies were incubated overnight, and secondary antibodies for 1 hr at 4 °C in blocking solution. DAPI (D9542, Sigma-Aldrich) was used as a counterstain to label nuclei. To detect apoptotic cells, Pax7 immunohistochemistry was combined with TUNEL TMR Red detection kit according to the manufacturer's instruction (12156792910, Roche). To monitor proliferating cells, EdU (50  $\mu$ g/g body weight) was given i.p. 2 hr before the isolation of the muscle. EdU was detected using Click chemistry (EdU-Click 647, BCK-EdU647, baseclick GmbH) and Biotin picolyl azide (900912, Sigma-Aldrich) as substrate. Detection was performed with fluorophore-coupled streptavidin. Images were acquired using a LSM700 confocal microscope and processed using Adobe Photoshop (Adobe Systems).

## Isolation of muscle stem cells and muscle injury

Muscle stem cells were isolated from skeletal muscle using fluorescent-activated cell sorting (FACS) as described (Bröhl *et al.*, 2012). Shortly, muscle tissue was minced, enzymatically digested with 1.5 U/ml NB4G Collagenase (S1745401, Serva), and 2.4 U/ml Dispase (04942078001, Sigma-Aldrich). Mono-nucleated cells were isolated and labeled with antibodies against VCAM, Sca1, CD45, CD31 (AF643, rndsystems; BD Bioscience). VCAM<sup>+</sup> Sca1<sup>+</sup> CD31<sup>+</sup> CD45<sup>+</sup> cells were isolated using a BD Aria III sorter (BD Bioscience) and dead cells were excluded by propidium iodide staining (P4864, Sigma-Aldrich). Muscle stem cells from regenerating muscles were isolated from animals carrying Pax7<sup>nGFP</sup> allele using the digestion procedure described above. Mono-nucleated cells GFP<sup>+</sup> cells were isolated by FACS. Cells were collected in TRIzol RNA extraction reagent (15596026, Thermo Fisher Scientific) for RNA isolation or in DMEM/10 % FCS for cultivation.

Muscle injury was induced by injecting 30  $\mu$ l of cardiotoxin (10  $\mu$ M; C9759, Sigma-Aldrich) into the *tibialis anterior* muscle of 8- to 12-week-old mice. Muscle injected with phosphate buffered saline (10010056, Thermo Fisher Scientific) was used as a control. Recombination using CreERT2 alleles was induced as described (Murphy *et al.*, 2011), and the injury was induced 10 days after the last tamoxifen administration. Antigen affinity-purified polyclonal goat human/mouse TNF $\alpha$  antibody (AF-410-NA, rndsystems, LOT NQ2519111, NQ2520111, NQ2418041) was dissolved in PBS and

100 µg were injected in a single injection i.p. 2 hr before the cardiotoxin injection. Mice injected with 100 µg goat IgG (AB-108-C, rndsystems) served as control. The animals were analyzed 4 days after injury.

### Mouse strains

The *Cxcr4*<sup>flox</sup>, *Met*<sup>flox</sup>, *Pax7*<sup>nGFP</sup>, *Pax7*<sup>iresCre</sup>, *Pax7*<sup>CreERT2Fan</sup>, and *Pax7*<sup>iresCreERT2Gaka</sup> mouse strains have been described previously (Borowiak et al., 2004; Keller et al., 2004; Nie et al., 2004; Lepper et al., 2009; Sambasivan et al., 2009; Murphy et al., 2011). Heterozygous animals carrying the *Pax7*<sup>iresCre</sup> allele served as controls for *Pax7*<sup>iresCre/+</sup>; *Met*<sup>flox/flox</sup> (coMet) mutants. Heterozygous animals carrying the *Pax7*<sup>iresCreERT2Gaka</sup> or *Pax7*<sup>CreERT2Fan</sup> treated with tamoxifen served as controls for *Pax7*<sup>iresCreERT2Gaka/+</sup>; *Met*<sup>flox/flox</sup> (*Tx*<sup>GakaMet</sup>) and *Pax7*<sup>CreERT2Fan/-</sup>; *Met*<sup>flox/flox</sup> (*Tx*<sup>FanMet</sup>) mutants, respectively, in all experiments but those shown in **Figure 3—figure supplement 1A–D**, where Cre-negative littermates served as controls. Mice were maintained on a mixed 129/Sv and C57BL/6 genetic background. All experiments were conducted according to regulations established by the Max-Delbrück-Center for Molecular Medicine (MDC) and the Landesamt für Gesundheit und Soziales, Berlin (0320/10; 0130/13).

### Cultivation, induction of apoptosis, and rescue of muscle stem cells in culture

Neutralization capacity of the TNFα antibody (AF-410-NA, rndsystems) was tested in vitro. C2C12 cells (ATCC, CRL-1772; not listed by ICLAC) in DMEM (1196508, Thermo Fisher Scientific) containing 2 % horse serum (16050122, Thermo Fisher Scientific), 1 % Penicillin/Streptomycin (15140122, Thermo Fisher Scientific), and 1 % GlutaMax (35050061, Thermo Fisher Scientific) were exposed to 60 ng/ml recombinant TNFα (210-TA, rndsystems) and different concentrations of TNFα neutralizing antibody (60 ng/ml, 180 ng/ml, 600 ng/ml, and 1800 ng/ml) overnight, fixed in 4 % paraformaldehyde (PFA), and apoptotic cells were detected using TUNEL TMR Red detection kit according to the manufacturer's instruction (12156792910, Roche). The ratio of TUNEL+ DAPI+/DAPI+ cells was quantified in randomly chosen areas of triplicate experiments using a LSM700 Zeiss confocal microscope and ImageJ 'cell counter' plug-in for quantification. The cell identity of the C2C12 cell line used in this study was tested by in vitro differentiation into multinuclear myotubes. Differentiation was achieved by replacing growth media (GM) (10 % fetal calf serum (FCS) F7524, Sigma-Aldrich, DMEM 1196508, Thermo Fisher Scientific, 1 % Penicillin/Streptomycin 15140122, Thermo Fisher Scientific, 1 % GlutaMax 35050061, Thermo Fisher Scientific) to differentiation media (DM) (2 % horse serum 16050122, Thermo Fisher Scientific, DMEM 1196508, Thermo Fisher Scientific, 1 % Penicillin/Streptomycin 15140122, Thermo Fisher Scientific, 1 % GlutaMax 35050061, Thermo Fisher Scientific). Formation of myotubes was observed 4 days after replacing the GM to DM. Differentiation was confirmed by immunohistochemistry using an antibody against Myogenin. The C2C12 cell line was tested negative for mycoplasma contamination.

FACS-isolated muscle stem cells were cultivated on 10 % Matrigel (354230, Corning Life Sciences) in DMEM/F-12 (11320074, Thermo Fisher Scientific) containing 10 % fetal calf serum (F7524, Sigma-Aldrich), 5 % horse serum (16050122, Thermo Fisher Scientific), 0.1 % bovine FGF (F5329, Sigma-Aldrich), 1 % Penicillin/Streptomycin (15140122, Thermo Fisher Scientific), and 1 % GlutaMax (35050061, Thermo Fisher Scientific) for 24 hr, and subsequently incubated in DMEM/F-12 containing 2 % horse serum. Recombinant human TNFα (210-TA, rndsystems) was added to a final concentration of 120 ng/ml, and cell survival was assayed 3 hr later. Recombinant Cxcl12 (250-20A, Peprotech) and HGF protein (kindly provided by W. Birchmeier) were used at final concentrations of 20 ng/ml and 25 ng/ml, respectively. After 3 hr incubation, cells were fixed in 4 % PFA and washed twice with phosphate-buffered saline (PBS) (10010056, Thermo Fisher Scientific). To detect apoptotic cells, *Pax7* immunohistochemistry was combined with TUNEL TMR Red detection according to the manufacturer's instruction (12156792910, Roche); DAPI (D9542, Sigma-Aldrich) was used as a counterstain. The ratio of TUNEL+ DAPI+/DAPI+ cells was quantified in randomly chosen areas of three different experiments using a LSM700 Zeiss confocal microscope and ImageJ 'cell counter' plug-in.

### Computational analysis and statistics

Gene expression levels of freshly isolated and cultured muscle stem cells were previously determined using gene expression microarrays (Liu et al., 2013; Latroche et al., 2017). The \*.CEL files of scanned

Affymetrix mRNA expression microarrays were downloaded from the GEO repository (accession codes GSE47177 and GSE103684,  $n = 3$  replicates/condition). Normalization and background corrections were performed using the AffySTExpressionCreator v0.14 on the GenePattern Server (Reich et al., 2006) running the Robust Multi-array Average (RMA) algorithm (Irizarry et al., 2003). The relative signal intensities of gene expression of muscle stem cell activation were plotted against the time axis.

Three or more animals were used per genotype and experiment. Microsoft Excel and GraphPad Prism 9 were used for statistical analysis. Data were analyzed using an unpaired, two-tailed t-test.  $p$ -values  $< 0.05$  were considered significant. Results are shown as arithmetical mean  $\pm$  standard error of the mean (SEM) and the dots represent the mean of individual animals. ns: not significant,  $p > 0.05$ , \* $p < 0.05$ , \*\* $p < 0.01$ , \*\*\* $p < 0.001$ .

## Acknowledgements

We thank Walter Birchmeier, Thomas Müller, and Minchul Kim for helpful discussions. We are grateful to Vivian Schulz, Pia Blessin, and Sven Buchert for technical assistance, and to Petra Stallerow and Claudia Päseler for help with the animal husbandry. We also acknowledge Elijah Lowenstein and Thomas Müller for critically reading the manuscript. This work was supported by the Deutsche Forschungsgemeinschaft (DFG, Klinische Forschergruppe KFO 192 and AFM/Telethon to CB).

---

## Additional information

### Competing interests

Jie-Shin Chen: Jie-Shin Chen is now affiliated with AstraZeneca; all work for this manuscript was conducted while affiliated with Max Delbrueck Center for Molecular Medicine (MDC) in the Helmholtz Society. The other authors declare that no competing interests exist.

### Funding

Funder	Grant reference number	Author
Deutsche Forschungsgemeinschaft		Carmen Birchmeier
AFM		Carmen Birchmeier
Klinische Forschergruppe KFO 192		Carmen Birchmeier

The funders had no role in study design, data collection and interpretation, or the decision to submit the work for publication.

### Author contributions

Ines Lahmann, Conceptualization, Investigation, Writing – original draft; Joscha Griger, Jie-Shin Chen, Yao Zhang, Investigation; Markus Schuelke, Computational analysis; Carmen Birchmeier, Conceptualization, Supervision, Writing – original draft

### Author ORCIDs

Carmen Birchmeier  <http://orcid.org/0000-0002-2041-8872>

### Ethics

All experiments were conducted according to regulations established by the Max-Delbrück- Center for Molecular Medicine (MDC) and the Landesamt für Gesundheit und Soziales (0320/10; 0130/13).

### Decision letter and Author response

Decision letter <https://doi.org/10.7554/eLife.57356.sa1>

Author response <https://doi.org/10.7554/eLife.57356.sa2>



## Additional files

### Supplementary files

- Supplementary file 1. *Tnf*, *Hgf*, and *Cxcl12* expression levels during muscle regeneration. Expression levels of *Tnf*, *Hgf*, and *Cxcl12* mRNA after acute injury were determined in the entire muscle by qPCR. Uninjured and 1–7 days post injury (dpi) were assessed, and expression was normalized to the expression in the uninjured muscle. The values are displayed as means  $\pm$  SEM. p-Values are shown in brackets.  $\beta$ -Actin was used for normalization.
- Transparent reporting form

### Data availability

All data generated or analysed during this study are included in the manuscript and supporting files.

## References

- Aggarwal BB.** 2003. Signalling pathways of the TNF superfamily: A double-edged sword. *Nature Reviews Immunology* **3**: 745–756. DOI: <https://doi.org/10.1038/nri1184>, PMID: 12949498
- Allen RE, Sheehan SM, Taylor RG, Kendall TL, Rice GM.** 1995. Hepatocyte growth factor activates quiescent skeletal muscle satellite cells in vitro. *Journal of Cellular Physiology* **165**: 307–312. DOI: <https://doi.org/10.1002/jcp.1041650211>, PMID: 7593208
- Birchmeier C, Birchmeier W, Gherardi E, Vande Woude GF.** 2003. Met, metastasis, motility and more. *Nature Reviews Molecular Cell Biology* **4**: 915–925. DOI: <https://doi.org/10.1038/nrm1261>, PMID: 14685170
- Bladt F, Riethmacher D, Isenmann S, Aguzzi A, Birchmeier C.** 1995. Essential role for the c-met receptor in the migration of myogenic precursor cells into the limb bud. *Nature* **376**: 768–771. DOI: <https://doi.org/10.1038/376768a0>, PMID: 7651534
- Bobadilla M, Sainz N, Abizanda G, Orbe J, Rodriguez JA, Páramo JA, Prósper F, Pérez-Ruiz A.** 2014. The cxcr4/sdf1 axis improves muscle regeneration through mmp-10 activity. *Stem Cells and Development* **23**: 1417–1427. DOI: <https://doi.org/10.1089/scd.2013.0491>, PMID: 24548137
- Borowiak M, Garratt AN, Wüstefeld T, Strehle M, Trautwein C, Birchmeier C.** 2004. Met provides essential signals for liver regeneration. *PNAS* **101**: 10608–10613. DOI: <https://doi.org/10.1073/pnas.0403412101>, PMID: 15249655
- Bröhl D, Vasyutina E, Czajkowski MT, Griger J, Rassek C, Rahn HP, Purfürst B, Wende H, Birchmeier C.** 2012. Colonization of the satellite cell niche by skeletal muscle progenitor cells depends on notch signals. *Developmental Cell* **23**: 469–481. DOI: <https://doi.org/10.1016/j.devcel.2012.07.014>, PMID: 22940113
- Butterfield TA, Best TM, Merrick MA.** 2006. The dual roles of neutrophils and macrophages in inflammation: A critical balance between tissue damage and repair. *Journal of Athletic Training* **41**: 457–465. DOI: [https://doi.org/10.1016/S0162-0908\(08\)79217-1](https://doi.org/10.1016/S0162-0908(08)79217-1), PMID: 17273473
- Chargé SBP, Rudnicki MA.** 2004. Cellular and molecular regulation of muscle regeneration. *Physiological Reviews* **84**: 209–238. DOI: <https://doi.org/10.1152/physrev.00019.2003>, PMID: 14715915
- Chazaud B, Brigitte M, Yacoub-Youssef H, Arnold L, Gherardi R, Sonnet C, Lafuste P, Chretien F.** 2009. Dual and beneficial roles of macrophages during skeletal muscle regeneration. *Exercise and Sport Sciences Reviews* **37**: 18–22. DOI: <https://doi.org/10.1097/JES.0b013e318190ebdb>, PMID: 19098520
- Collins RA, Grounds MD.** 2001. The role of tumor necrosis factor-alpha (TNF-alpha) in skeletal muscle regeneration Studies in TNF-alpha(-/-) and TNF-alpha(-)/LT-alpha(-/-) mice. *The Journal of Histochemistry and Cytochemistry* **49**: 989–1001. DOI: <https://doi.org/10.1177/002215540104900807>, PMID: 11457927
- Cornelison DD, Wold BJ.** 1997. Single-cell analysis of regulatory gene expression in quiescent and activated mouse skeletal muscle satellite cells. *Developmental Biology* **191**: 270–283. DOI: <https://doi.org/10.1006/dbio.1997.8721>, PMID: 9398440
- Cornelison DDW.** 2008. Context matters: In vivo and in vitro influences on muscle satellite cell activity. *Journal of Cellular Biochemistry* **105**: 663–669. DOI: <https://doi.org/10.1002/jcb.21892>, PMID: 18759329
- Darnay BG, Aggarwal BB.** 1999. Signal transduction by tumour necrosis factor and tumour necrosis factor related ligands and their receptors. *Annals of the Rheumatic Diseases* **58 Suppl 1**: I2–I13. DOI: <https://doi.org/10.1136/ard.58.2008.i2>, PMID: 10577967
- Franke TF, Hornik CP, Segev L, Shostak GA, Sugimoto C.** 2003. PI3K/AKT and Apoptosis: Size matters. *Oncogene* **22**: 8983–8998. DOI: <https://doi.org/10.1038/sj.onc.1207115>, PMID: 14663477
- Gal-Levi R, Leshem Y, Aoki S, Nakamura T, Halevy O.** 1998. Hepatocyte growth factor plays a dual role in regulating skeletal muscle satellite cell proliferation and differentiation. *Biochimica et Biophysica Acta* **1402**: 39–51. DOI: [https://doi.org/10.1016/s0167-4889\(97\)00124-9](https://doi.org/10.1016/s0167-4889(97)00124-9), PMID: 9551084
- Gentile A, Trusolino L, Comoglio PM.** 2008. The met tyrosine kinase receptor in development and cancer. *Cancer Metastasis Reviews* **27**: 85–94. DOI: <https://doi.org/10.1007/s10555-007-9107-6>, PMID: 18175071
- Griffin CA, Apponi LH, Long KK, Pavlath GK.** 2010. Chemokine expression and control of muscle cell migration during myogenesis. *Journal of Cell Science* **123**: 3052–3060. DOI: <https://doi.org/10.1242/jcs.066241>, PMID: 20736301
- Hardy D, Besnard A, Latil M, Jouvion G, Briand D, Thépenier C, Pascal Q, Guguin A, Gayraud-Morel B, Cavaillon J-M, Tajbakhsh S, Rocheteau P, Chretien F.** 2016. Comparative study of injury models for studying

- muscle regeneration in mice. *PLOS ONE* 11: e0147198. DOI: <https://doi.org/10.1371/journal.pone.0147198>, PMID: 26807982
- Hirata A, Masuda S, Tamura T, Kai K, Ojima K, Fukase A, Motoyoshi K, Kamakura K, Miyagoe-Suzuki Y, Takeda S. 2003. Expression profiling of cytokines and related genes in regenerating skeletal muscle after cardiotoxin injection: A role for osteopontin. *The American Journal of Pathology* 163: 203–215. DOI: [https://doi.org/10.1016/S0002-9440\(10\)63644-9](https://doi.org/10.1016/S0002-9440(10)63644-9), PMID: 12819025
- Irizarry RA, Hobbs B, Collin F, Beazer-Barclay YD, Antonellis KJ, Scherf U, Speed TP. 2003. Exploration, normalization, and summaries of high density oligonucleotide array probe level data. *Biostatistics* 4: 249–264. DOI: <https://doi.org/10.1093/biostatistics/4.2.249>, PMID: 12925520
- Järvinen TAH, Järvinen TLN, Kääriäinen M, Kalimo H, Järvinen M. 2005. Muscle injuries: Biology and treatment. *The American Journal of Sports Medicine* 33: 745–764. DOI: <https://doi.org/10.1177/0363546505274714>, PMID: 15851777
- Keller C, Hansen MS, Coffin CM, Capecchi MR. 2004. Pax3:Fkhr interferes with embryonic Pax3 and Pax7 function: implications for alveolar rhabdomyosarcoma cell of origin. *Genes & Development* 18: 2608–2613. DOI: <https://doi.org/10.1101/gad.1243904>, PMID: 15520281
- Kharraz Y, Guerra J, Pessina P, Serrano AL, Muñoz-Cánoves P. 2014. Understanding the process of fibrosis in Duchenne muscular dystrophy. *BioMed Research International* 2014: 965631. DOI: <https://doi.org/10.1155/2014/965631>, PMID: 24877152
- Latroche C, Weiss-Gayet M, Muller L, Gitiaux C, Leblanc P, Liot S, Ben-Larbi S, Abou-Khalil R, Verger N, Bardot P, Magnan M, Chrétien F, Mounier R, Germain S, Chazaud B. 2017. Coupling between myogenesis and angiogenesis during skeletal muscle regeneration is stimulated by restorative macrophages. *Stem Cell Reports* 9: 2018–2033. DOI: <https://doi.org/10.1016/j.stemcr.2017.10.027>, PMID: 29198825
- Lau KS, Juchheim AM, Cavaliere KR, Philips SR, Lauffenburger DA, Haigis KM. 2011. In vivo systems analysis identifies spatial and temporal aspects of the modulation of TNF- $\alpha$ -induced apoptosis and proliferation by MAPKs. *Science Signaling* 4: ra16. DOI: <https://doi.org/10.1126/scisignal.2001338>, PMID: 21427409
- Le Moal E, Pialoux V, Juban G, Groussard C, Zouhal H, Chazaud B, Mounier R. 2017. Redox control of skeletal muscle regeneration. *Antioxidants & Redox Signaling* 27: 276–310. DOI: <https://doi.org/10.1089/ars.2016.6782>, PMID: 28027662
- Lepper C, Conway SJ, Fan CM. 2009. Adult satellite cells and embryonic muscle progenitors have distinct genetic requirements. *Nature* 460: 627–631. DOI: <https://doi.org/10.1038/nature08209>, PMID: 19554048
- Li Y-P. 2003. TNF- $\alpha$  is a mitogen in skeletal muscle. *American Journal of Physiology-Cell Physiology* 285: C370–C376. DOI: <https://doi.org/10.1152/ajpcell.00453.2002>
- Liu L, Cheung TH, Charville GW, Hurgo BMC, Leavitt T, Shih J, Brunet A, Rando TA. 2013. Chromatin modifications as determinants of muscle stem cell quiescence and chronological aging. *Cell Reports* 4: 189–204. DOI: <https://doi.org/10.1016/j.celrep.2013.05.043>, PMID: 23810552
- Londhe P, Guttridge DC. 2015. Inflammation induced loss of skeletal muscle. *Bone* 80: 131–142. DOI: <https://doi.org/10.1016/j.bone.2015.03.015>, PMID: 26453502
- Lu Z, Xu S. 2006. Erk1/2 map kinases in cell survival and apoptosis. *IUBMB Life* 58: 621–631. DOI: <https://doi.org/10.1080/15216540600957438>, PMID: 17085381
- Luo JL, Kamata H, Karin M. 2005. Ikk/nf-kappab signaling: Balancing life and death—a new approach to cancer therapy. *The Journal of Clinical Investigation* 115: 2625–2632. DOI: <https://doi.org/10.1172/JCI26322>, PMID: 16200195
- Mademtoglou D, Asakura Y, Borok MJ, Alonso-Martin S, Mourikis P, Kodaka Y, Mohan A, Asakura A, Relaix F. 2018. Cellular localization of the cell cycle inhibitor cDkn1C controls growth arrest of adult skeletal muscle stem cells. *eLife* 7: e33337. DOI: <https://doi.org/10.7554/eLife.33337>, PMID: 30284969
- Malka D, Vasseur S, Bödeker H, Ortiz EM, Dusetti NJ, Verrando P, Dagorn JC, Iovanna JL. 2000. Tumor necrosis factor Alpha triggers antiapoptotic mechanisms in rat pancreatic cells through pancreatitis-associated protein 1 activation. *Gastroenterology* 119: 816–828. DOI: <https://doi.org/10.1053/gast.2000.16491>, PMID: 10982776
- Mann CJ, Perdiguero E, Kharraz Y, Aguilar S, Pessina P, Serrano AL, Muñoz-Cánoves P. 2011. Aberrant repair and fibrosis development in skeletal muscle. *Skeletal Muscle* 1: 21. DOI: <https://doi.org/10.1186/2044-5040-1-21>, PMID: 21798099
- Matsumoto K, Nakamura T. 2001. Hepatocyte growth factor: Renotropic role and potential therapeutics for renal diseases. *Kidney International* 59: 2023–2038. DOI: <https://doi.org/10.1046/j.1523-1755.2001.00717.x>, PMID: 11380804
- Matsumoto K, Funakoshi H, Takahashi H, Sakai K. 2014. HGF-Met Pathway in Regeneration and Drug Discovery. *Biomedicines* 2: 275–300. DOI: <https://doi.org/10.3390/biomedicines2040275>, PMID: 28548072
- Mauro A. 1961. Satellite cell of skeletal muscle fibers. *The Journal of Biophysical and Biochemical Cytology* 9: 493–495. DOI: <https://doi.org/10.1083/jcb.9.2.493>, PMID: 13768451
- Michalopoulos GK, DeFrances MC. 1997. Liver regeneration. *Science* 276: 60–66. DOI: <https://doi.org/10.1126/science.276.5309.60>, PMID: 9082986
- Miller KJ, Thaloor D, Matteson S, Pavlath GK. 2000. Hepatocyte growth factor affects satellite cell activation and differentiation in regenerating skeletal muscle. *American Journal of Physiology-Cell Physiology* 278: C174–C181. DOI: <https://doi.org/10.1152/ajpcell.2000.278.1.C174>
- Murphy MM, Lawson JA, Mathew SJ, Hutcheson DA, Kardon G. 2011. Satellite cells, connective tissue fibroblasts and their interactions are crucial for muscle regeneration. *Development* 138: 3625–3637. DOI: <https://doi.org/10.1242/dev.064162>, PMID: 21828091

- Nakamura T**, Mizuno S, Matsumoto K, Sawa Y, Matsuda H, Nakamura T. 2000. Myocardial protection from ischemia/reperfusion injury by endogenous and exogenous HGF. *The Journal of Clinical Investigation* **106**: 1511–1519. DOI: <https://doi.org/10.1172/JCI10226>, PMID: 11120758
- Nakamura T**, Mizuno S. 2010. The discovery of hepatocyte growth factor (HGF) and its significance for cell biology, life sciences and clinical medicine. *PNAS* **86**: 588–610. DOI: <https://doi.org/10.2183/pjab.86.588>, PMID: 20551596
- Nie Y**, Waite J, Brewer F, Sunshine MJ, Littman DR, Zou YR. 2004. The role of CXCR4 in maintaining peripheral b cell compartments and humoral immunity. *The Journal of Experimental Medicine* **200**: 1145–1156. DOI: <https://doi.org/10.1084/jem.20041185>, PMID: 15520246
- Odemis V**, Boosmann K, Dieterlen MT, Engele J. 2007. The chemokine SDF1 controls multiple steps of myogenesis through atypical PKCZETA. *Journal of Cell Science* **120**: 4050–4059. DOI: <https://doi.org/10.1242/jcs.010009>, PMID: 17971416
- Palacios D**, Mozzetta C, Consalvi S, Caretti G, Saccone V, Proserpio V, Marquez VE, Valente S, Mai A, Forcales SV, Sartorelli V, Puri PL. 2010. TNF/p38 $\alpha$ /polycomb signaling to Pax7 locus in satellite cells links inflammation to the epigenetic control of muscle regeneration. *Cell Stem Cell* **7**: 455–469. DOI: <https://doi.org/10.1016/j.stem.2010.08.013>, PMID: 20887952
- Pang Y**, Liang M-T, Gong Y, Yang Y, Bu P-L, Zhang M, Yao H-C. 2018. HGF Reduces Disease Severity and Inflammation by Attenuating the NF- $\kappa$ B Signaling in a Rat Model of Pulmonary Artery Hypertension. *Inflammation* **41**: 924–931. DOI: <https://doi.org/10.1007/s10753-018-0747-1>, PMID: 29442198
- Reich M**, Liefeld T, Gould J, Lerner J, Tamayo P, Mesirov JP. 2006. Genepattern 2.0. *Nature Genetics* **38**: 500–501. DOI: <https://doi.org/10.1038/ng0506-500>, PMID: 16642009
- Relaix F**, Rocancourt D, Mansouri A, Buckingham M. 2004. Divergent functions of murine pax3 and pax7 in limb muscle development. *Genes & Development* **18**: 1088–1105. DOI: <https://doi.org/10.1101/gad.301004>, PMID: 15132998
- Relaix F**, Zammit PS. 2012. Satellite cells are essential for skeletal muscle regeneration: The cell on the edge returns centre stage. *Development* **139**: 2845–2856. DOI: <https://doi.org/10.1242/dev.069088>, PMID: 22833472
- Rodgers JT**, King KY, Brett JO, Cromie MJ, Charville GW, Maguire KK, Brunson C, Mastey N, Liu L, Tsai CR, Goodell MA, Rando TA. 2014. mTORC1 controls the adaptive transition of quiescent stem cells from G0 to G(Alert). *Nature* **510**: 393–396. DOI: <https://doi.org/10.1038/nature13255>, PMID: 24870234
- Sacliier M**, Cuvellier S, Magnan M, Mounier R, Chazaud B. 2013a. Monocyte/macrophage interactions with myogenic precursor cells during skeletal muscle regeneration. *The FEBS Journal* **280**: 4118–4130. DOI: <https://doi.org/10.1111/febs.12166>, PMID: 23384231
- Sacliier M**, Yacoub-Youssef H, Mackey AL, Arnold L, Ardjoune H, Magnan M, Sailhan F, Chelly J, Pavlath GK, Mounier R, Kjaer M, Chazaud B. 2013b. Differentially activated macrophages orchestrate myogenic precursor cell fate during human skeletal muscle regeneration. *Stem Cells* **31**: 384–396. DOI: <https://doi.org/10.1002/stem.1288>, PMID: 23169615
- Sambasivan R**, Gayraud-Morel B, Dumas G, Cimper C, Paisant S, Kelly RG, Kelly R, Tajbakhsh S. 2009. Distinct regulatory cascades govern extraocular and pharyngeal arch muscle progenitor cell fates. *Developmental Cell* **16**: 810–821. DOI: <https://doi.org/10.1016/j.devcel.2009.05.008>, PMID: 19531352
- Seale P**, Sabourin LA, Girgis-Gabardo A, Mansouri A, Gruss P, Rudnicki MA. 2000. PAX7 is required for the specification of myogenic satellite cells. *Cell* **102**: 777–786. DOI: [https://doi.org/10.1016/s0092-8674\(00\)00066-0](https://doi.org/10.1016/s0092-8674(00)00066-0), PMID: 11030621
- Shimomura T**, Miyazawa K, Komiyama Y, Hiraoka H, Naka D, Morimoto Y, Kitamura N. 1995. Activation of hepatocyte growth factor by two homologous proteases, blood-coagulation factor XIIA and hepatocyte growth factor activator. *European Journal of Biochemistry* **229**: 257–261. DOI: <https://doi.org/10.1111/j.1432-1033.1995.tb20463.x>, PMID: 7744037
- Siegel AL**, Atchison K, Fisher KE, Davis GE, Cornelison DD. 2009. 3D timelapse analysis of muscle satellite cell motility. *Stem Cells* **27**: 2527–2538. DOI: <https://doi.org/10.1002/stem.178>, PMID: 19609936
- Tatsumi R**, Anderson JE, Nevoret CJ, Halevy O, Allen RE. 1998. HGF/SF is present in normal adult skeletal muscle and is capable of activating satellite cells. *Dev Biol* **194**: 114–128. DOI: <https://doi.org/10.1006/dbio.1997.8803>, PMID: 9473336
- Teicher BA**, Fricker SP. 2010. CXCL12 (SDF-1)/CXCR4 pathway in cancer. *Clinical Cancer Research* **16**: 2927–2931. DOI: <https://doi.org/10.1158/1078-0432.CCR-09-2329>, PMID: 20484021
- Tidball JG**. 2005. Inflammatory processes in muscle injury and repair. *American Journal of Physiology-Regulatory, Integrative and Comparative Physiology* **288**: R345–R353. DOI: <https://doi.org/10.1152/ajpregu.00454.2004>
- Tidball JG**. 2017. Regulation of muscle growth and regeneration by the immune system. *Nature Reviews Immunology* **17**: 165–178. DOI: <https://doi.org/10.1038/nri.2016.150>, PMID: 28163303
- Tidball JG**, Welc SS, Wehling-Henricks M. 2018. Immunobiology of inherited muscular dystrophies. *Comprehensive Physiology* **8**: 1313–1356. DOI: <https://doi.org/10.1002/cphy.c170052>, PMID: 30215857
- Tran SE**, Holmstrom TH, Ahonen M, Kahari VM, Eriksson JE. 2001. MAPK/ERK overrides the apoptotic signaling from FAS, TNF, and trail receptors. *The Journal of Biological Chemistry* **276**: 16484–16490. DOI: <https://doi.org/10.1074/jbc.M010384200>, PMID: 11278665
- Turner MD**, Nedjai B, Hurst T, Pennington DJ. 2014. Cytokines and chemokines: At the crossroads of cell signalling and inflammatory disease. *Biochimica et Biophysica Acta* **1843**: 2563–2582. DOI: <https://doi.org/10.1016/j.bbamcr.2014.05.014>, PMID: 24892271



- Ueda H**, Sawa Y, Matsumoto K, Kitagawa-Sakakida S, Kawahira Y, Nakamura T, Kaneda Y, Matsuda H. 1999. Gene transfection of hepatocyte growth factor attenuates reperfusion injury in the heart. *The Annals of Thoracic Surgery* **67**: 1726–1731. DOI: [https://doi.org/10.1016/s0003-4975\(99\)00279-9](https://doi.org/10.1016/s0003-4975(99)00279-9), PMID: 10391282
- Vasyutina E**, Stebler J, Brand-Saberi B, Schulz S, Raz E, Birchmeier C. 2005. CXCR4 and gab1 cooperate to control the development of migrating muscle progenitor cells. *Genes & Development* **19**: 2187–2198. DOI: <https://doi.org/10.1101/gad.346205>, PMID: 16166380
- von Maltzahn J**, Jones AE, Parks RJ, Rudnicki MA. 2013. PAX7 is critical for the normal function of satellite cells in adult skeletal muscle. *PNAS* **110**: 16474–16479. DOI: <https://doi.org/10.1073/pnas.1307680110>, PMID: 24065826
- Wada T**, Penninger JM. 2004. Mitogen-activated protein kinases in apoptosis regulation. *Oncogene* **23**: 2838–2849. DOI: <https://doi.org/10.1038/sj.onc.1207556>, PMID: 15077147
- Wallach D**, Varfolomeev EE, Malinin NL, Goltsev YV, Kovalenko AV, Boldin MP. 1999. Tumor necrosis factor receptor and fas signaling mechanisms. *Annual Review of Immunology* **17**: 331–367. DOI: <https://doi.org/10.1146/annurev.immunol.17.1.331>, PMID: 10358762
- Warren GL**, Hulderman T, Jensen N, McKinstry M, Mishra M, Luster MI, Simeonova PP. 2002. Physiological role of tumor necrosis factor alpha in traumatic muscle injury. *FASEB Journal* **16**: 1630–1632. DOI: <https://doi.org/10.1096/fj.02-0187fje>, PMID: 12207010
- Webster MT**, Fan CM. 2013. c-MET regulates myoblast motility and myocyte fusion during adult skeletal muscle regeneration. *PLOS ONE* **8**: e81757. DOI: <https://doi.org/10.1371/journal.pone.0081757>, PMID: 24260586
- Xiao F**, Wang H, Fu X, Li Y, Ma K, Sun L, Gao X, Wu Z. 2011. Oncostatin m inhibits myoblast differentiation and regulates muscle regeneration. *Cell Research* **21**: 350–364. DOI: <https://doi.org/10.1038/cr.2010.144>, PMID: 20956996
- Zador E**, Mendler L, Takacs V, de Bleecker J, Wuytack F. 2001. Regenerating soleus and extensor digitorum longus muscles of the rat show elevated levels of TNF-alpha and its receptors, TNFR-60 and TNFR-80. *Muscle Nerve* **24**: 1058–1067. DOI: <https://doi.org/10.1002/mus.1110>, PMID: 11439381
- Zhou D**, Tan RJ, Lin L, Zhou L, Liu Y. 2013. Activation of hepatocyte growth factor receptor, C-met, in renal tubules is required for renoprotection after acute kidney injury. *Kidney International* **84**: 509–520. DOI: <https://doi.org/10.1038/ki.2013.102>, PMID: 23715119